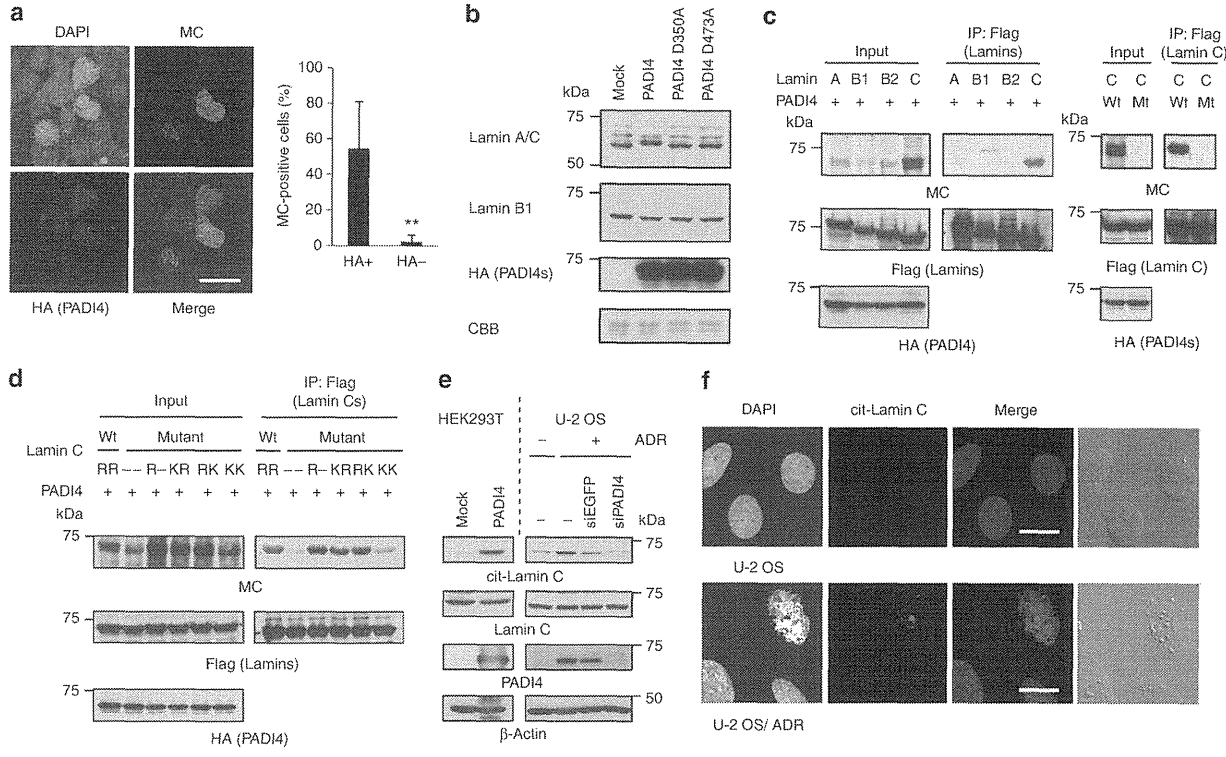

Figure 5 | Lamin C is citrullinated during nuclear fragmentation. (**a**) Representative image of HA-PADI4-transfected HEK293T cells stained with anti-modified citrulline (MC) antibody (Alexa Fluor 488) and anti-HA antibody (Aleza Fluor 594) (left panel). The proportion of MC-positive cells stratified by HA-PADI4 expression was indicated (right panel). Error bars represent s.d. ($n=9$). $^{**}P<0.01$ by Student's t-test. Scale bars, 20 μm. Cells were incubated with 5 μmol l^{-1} of A23187 for 1 h before fixation. (**b**) Western blotting for nuclear extracts from HEK293T cells transfected with wild-type PADI4, mutant PADI4 (D350A or D473A), or mock plasmid using each anti-Lamin antibody. (**c**) HEK293T cells were transfected with the indicated plasmids. Cell extracts were immunoprecipitated using anti-Flag antibody, followed by immunoblotting with anti-MC, anti-Flag, or anti-HA antibody. (**d**) HEK293T cells were transfected with the indicated plasmids. Cell extracts were immunoprecipitated using anti-Flag antibody, followed by immunoblotting with anti-MC, anti-Flag, or anti-HA antibody. (**e**) Whole-cell extracts from PADI4-transfected HEK293T cells or ADR-treated U-2 OS cells were subjected to western blotting using antibody against citrullinated Lamin C at arginine 571 and arginine 572 residues (cit-Lamin C), Lamin C, PADI4, or β-actin. Each siRNA was transfected 10 h before DNA damage treatment. siEGFP was used as a control. (**f**) Representative image of ADR-treated U-2 OS cells stained with anti-cit-Lamin C antibody (Alexa Fluor 488). Scale bars, 20 μm.

patients without cit-H4R3 expression (52.7%), although the difference was not statistically significant ($P=0.24$ by log-rank test; Fig. 7d). As many of p53 mutations lead to a prolonged half-life of p53 protein, immunohistochemistry of p53 is commonly used to detect p53 mutations in various cancers[24,25]. Interestingly, the positive p53 staining was inversely associated with cit-H4R3 staining ($P=0.0079$ by Student's t-test), indicating the regulation of chromatin modification by p53 in human carcinogenesis (Table 1).

Discussion

Accumulating evidence indicate that a combination of genetic and epigenetic alterations contribute to the development and progression of human cancers[26]. Among many genes altered in cancer tissues, the p53 gene was mutated in nearly half of all tumours[27–29]; however, the roles of p53 in histone modifications and chromatin structure have not been characterized. Here we clearly demonstrated the crucial roles of p53–PADI4 pathway in citrullination of H4R3 and Lamin C in response to DNA damage as well as in nuclear fragmentation.

A certain type or a combination of histone modifications termed as 'histone code'[30] are translated into a meaningful biological outcome such as gene expression and chromatin structure. Histone H2AX is phosphorylated at serine 139 residue (γ-H2AX) on external damage, and recruits DNA repair complex to promote chromatin remodelling[31,32]. Recently, phosphorylation of serine 14 residue in H2B, which was induced on several apoptotic stimuli including DNA damage[33], was proposed as a 'death code, but its physiological significance remains to be determined. Histone methylation, phosphorylation and acetylation are reversible processes that are regulated by histone-modifying enzymes[34]. In contrast, citrullination is a chemically stable modification, and decitrullination enzymes have not yet been discovered[35]. Therefore, histone citrullination is considered to be an irreversible cellular process. As histone H4 citrullination is associated with apoptosis of damaged cells as well as neutrophilic death triggered by NET formation, histone H4 citrullination could be defined as a functional apoptotic histone code.

Li *et al.* previously reported that PADI4 negatively regulated the $p21^{WAF1}$ expression through the interaction with p53 at a *p21*^{WAF1} promoter region in ultraviolet-irradiated U-2 OS cells[36]. In addition, PADI4 was shown to be transactivated in various cancer tissues[37], and siPADI4 or PADI4 inhibitor (Cl-amidine) suppressed proliferation of U-2 OS cells[36], suggesting PADI4 to function as an oncogene. However, the frequent inactivating mutations of *PADI4* in cancer cell lines as well as apoptosis-resistance in *Padi4*-null mice implied the possible role of PADI4 as a tumour suppressor. This discrepancy could be partially due to the difference in the experimental conditions. We analysed the effects of PADI4 knockdown using irradiated mice or ADR-treated cells, whereas Li *et al.* analysed U-2 OS cells under the non-stress condition or after ultraviolet treatment.

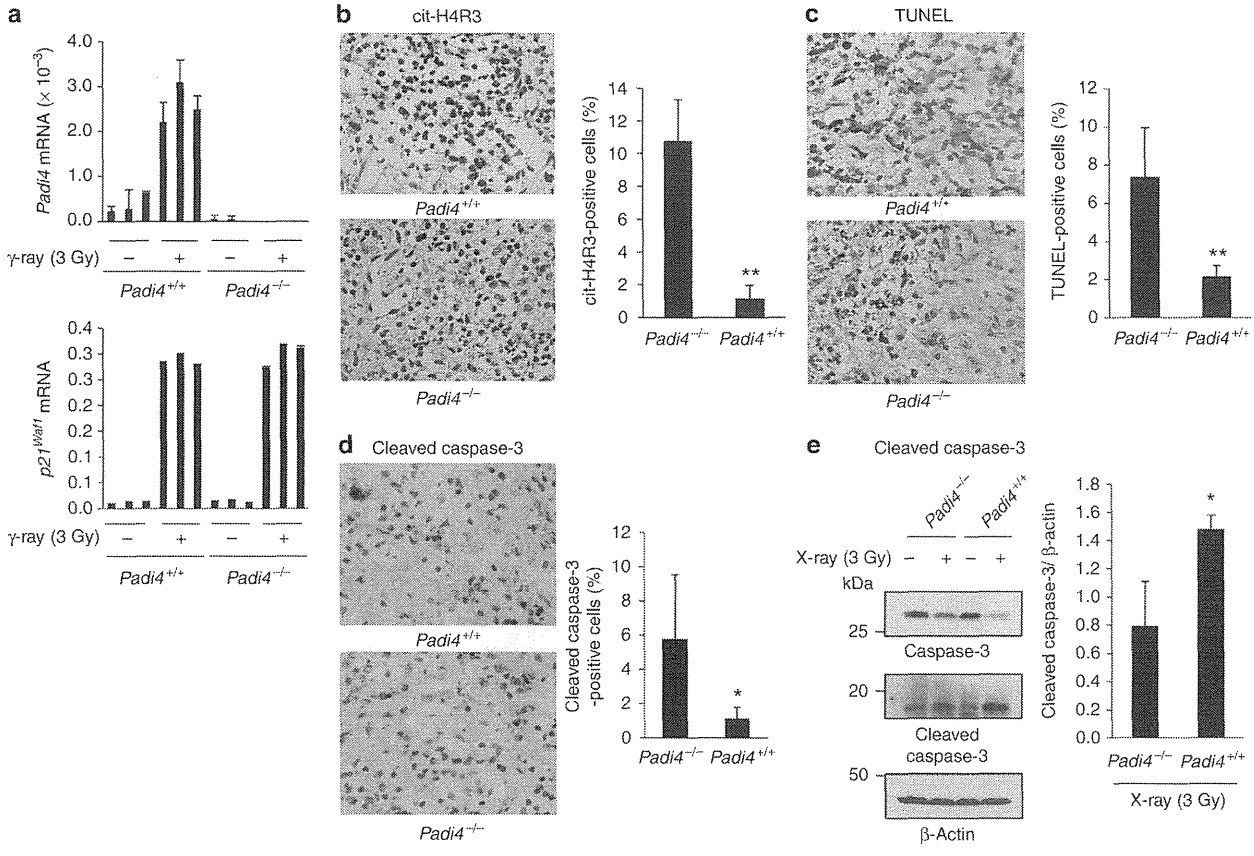

Figure 6 | The role of Padi4 in DNA damage induced apoptosis *in vivo*. (**a**) Quantitative real-time PCR analysis of *Padi4* and $p21^{Waf1}$ expression in thymuses from γ-ray-irradiated $Padi4^{-/-}$ or $Padi4^{+/+}$ mice (3 Gy). Error bars represent range ($n=2$). *Gapdh* was used for normalization of *Padi4* expression levels. Mice were sacrificed 24 h after irradiation with 3 Gy of γ-ray. (**b**) Representative images of thymus sections from γ-ray-irradiated $Padi4^{-/-}$ or $Padi4^{+/+}$ mouse 24 h after irradiation with 3 Gy of γ-ray stained for citrullinated histone H4R3 (cit-H4R3) (left panel, X40). The proportion of positive cells in $Padi4^{-/-}$ or $Padi4^{+/+}$ mouse was indicated (right panel). Error bars represent s.d. ($n=4$). $^{**}P<0.01$ by Student's *t*-test. (**c**) Representative images of TUNEL staining for thymus sections from γ-ray-irradiated $Padi4^{-/-}$ or $Padi4^{+/+}$ mouse 24 h after irradiation with 3 Gy of γ-ray (left panel, X40). The proportion of positive cells in $Padi4^{-/-}$ or $Padi4^{+/+}$ mouse was indicated (right panel). Error bars represent s.d. ($n=4$). $^{**}P<0.01$ by Student's *t*-test. (**d**) Representative images of cleaved-caspase-3 staining in thymus sections from γ-ray-irradiated $Padi4^{-/-}$ or $Padi4^{+/+}$ mouse 24 h after irradiation with 3 Gy of γ-ray (left panel, X40). The proportion of positive cells in $Padi4^{-/-}$ or $Padi4^{+/+}$ mouse was indicated (right panel). Error bars represent s.d. ($n=4$). $^{*}P<0.05$ by Student's *t*-test. (**e**) Whole-cell extracts of thymus from X-ray-irradiated $Padi4^{-/-}$ or $Padi4^{+/+}$ mice were subjected to immunoblotting with anti-cleaved caspase-3, anti-caspase-3 or anti-β-actin antibody (left panel). Mice were sacrificed 48 h after irradiation with 3 Gy of X-ray. The ratio between cleaved caspase-3 and β-actin from independent samples ($n=4$ for $Padi4^{-/-}$ mice and $n=2$ for $Padi4^{+/+}$ mice) was indicated (right panel). $^{*}P<0.05$ by Student's *t*-test.

Although ADR- or γ-ray-treatment remarkably increased PADI4 expression, ultraviolet-treatment did not induce *PADI4* expression in U-2 OS cells (Supplementary Fig. S8a). In addition, expression levels of $p21^{Waf1}$ in thymus in the $Padi4^{+/+}$ and $Padi4^{-/-}$ mice after γ-ray irradiation were not significantly different (Fig. 6a). Similarly, siPADI4 treatment did not affect the expression of p53-target genes including $p21^{WAF1}$ in ADR-treated U-2 OS cells (Supplementary Fig. S8b). Moreover, siPADI4-treated U373MG cells exhibited resistance to p53-induced apoptosis (Supplementary Fig. S8c). In fact, we observed the citrullination of histone H4R3 in 51.5% of lung cancer tissues, suggesting the activation of PADI4 in a large proportion of cancer tissues, as suggested in the previous report[37]. However, cancer tissues are persistently exposed to oxidative stress compared with adjacent normal tissues[38,39], activation of PADI4 would be related with cellular stress condition. Taken together, we assume that PADI4 could predominantly function as a tumour suppressor that mediates the apoptotic process of damaged cells.

Although the molecular mechanism of how PADI4 increases DNA accessibility was not fully elucidated, loss of positive charge by citrullination was shown to induce conformational changes of histone H4 N terminal[40]. DNA–histone interaction is charge-dependent, and changes in the charge of the histone tails are considered to weaken histone-DNA interaction[41]. Moreover, we found that the interaction between core histones and nucleophosmin was inhibited by citrullination (Supplementary Fig. S8d). Any or all of these changes can affect the structure and folding of individual nucleosome that could lead to a more open and permissive chromatin environment. The role of PADI4 in chromatin remodelling was shown in the previous papers[42,43]. We also reported that DNA damage induced PADI4 expression and the citrullination of various proteins in our previous study[10]. To our knowledge, this is the first report demonstrating the important role of histone H4R3 citrullination in human carcinogenesis and the p53-mediated apoptotic pathway.

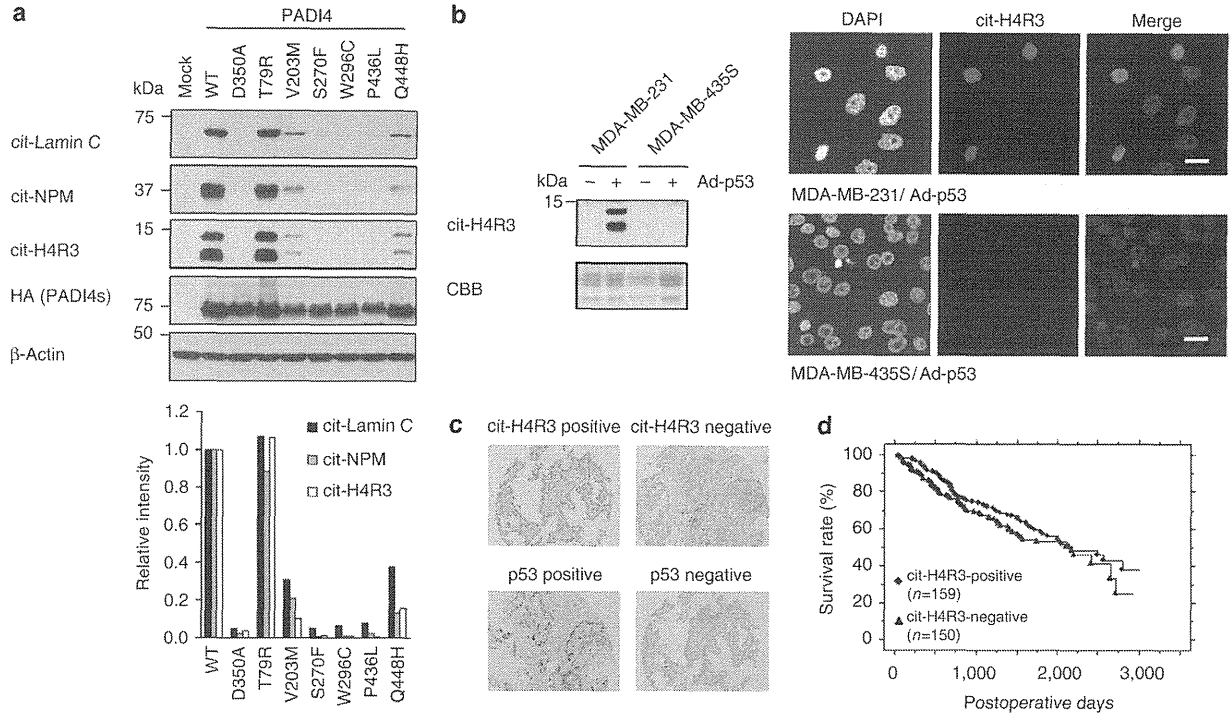

Figure 7 | Involvement of PADI4 in carcinogenesis. (**a**) Whole-cell extracts from HEK293T cells transfected with wild-type or mutant PADI4 were subjected to western blotting using anti-citrullinated Lamin C (cit-Lamin C), anti-citrullinated nucleophosmin (cit-NPM), anti-citrullinated histone H4R3 (cit-H4R3), anti-HA, or anti-β-actin antibody (upper panel). For quantification, band intensities were normalized to the signal in cells transfected with wild-type PADI4 (lower panel). (**b**) MDA-MB-231 and MDA-MB-435S cells were infected with adenovirus vector expressing p53 (Ad-p53). Histones were subjected to western blotting using anti-cit-H4R3 (left panel). Representative images of Ad-p53-infected cells stained for cit-H4R3 is shown in right panel. Scale bars, 20 μm. (**c**) cit-H4R3 or p53 expression in NSCLC tissues (magnification X10). (**d**) Kaplan–Meier analysis of survival in patients with NSCLC according to the expression of cit-H4R3 ($P = 0.24$, log-rank test).

Methods

Cell culture and transfections. Cell lines were purchased from American Type Culture Collection, Lonza Biologics, or Japanese Collection of Research Bioresources. Cells were transfected with plasmids using FuGENE6 (Roche). Replication-deficient recombinant viruses Ad-p53 or Ad-LacZ, expressing p53 or LacZ, respectively, were generated and purified, as described previously[5]. siRNA oligonucleotides, commercially synthesized by Sigma Genosys, were transfected with Lipofectamine RNAiMAX reagent or Lipofectamine 2000 reagent (Invitrogen). Sequences of oligonucleotides are shown in Supplementary Table S3. For treatment with calcium ionophore, cells were incubated with 5 μM of A23187 (Calbiochem) for 1 h at 37 °C.

Plasmid construction. Complementary DNA fragments of Lamin A, Lamin B1, Lamin B2 and Lamin C were amplified and cloned into pCAGGS vector. PADI4 expression plasmids were previously described[10]. Plasmids expressing mutant PADI4 or Lamin C were generated using the inverse PCR methods or by using the reverse primer containing point mutation at either or both of arginine 571 and 572 residues, respectively. The primer sequences for cloning and mutagenesis are shown in Supplementary Table S3.

Knockout mice. We amplified a 5,837 bp fragment containing exon 1 and exon 2 of *Padi4* using C57BL/6 genomic DNA as a template. The targeting vector was designed to replace exon 1 and 2, including the transcription initiation site, by mouse PGK-1 promoter and the neomycin-resistance gene (Supplementary Fig. S5a). We introduced the linearized targeting vector by electroporation into embryonic stem cells, and identified two independent targeted 129S1 embryonic stem cell clones by Southern blot analysis. We generated chimeric males by the aggregation method and crossed them with C57BL/6 females, and verified germline transmission by Southern blot analysis (Supplementary Fig. S5b,c). All *Padi4*$^{-/-}$ mice used in this study had been backcrossed for ten generations into the C57BL/6 background. We used RT–PCR to determine the presence of the *Padi4* transcript (Supplementary Fig. S5d). p53-deficient mice were provided from RIKEN BioResource Center (Ibaragi, Japan)[44]. Genotypes were confirmed by PCR analysis. The primer sequences are indicated in Supplementary Table S3. All mice were maintained under specific pathogen-free conditions and were handled in accordance with the Guidelines for Animal Experiments of the Institute of Medical Science (University of Tokyo, Tokyo, Japan).

DNA damaging treatment. For treatment with genotoxic stress, cells were continuously incubated with 2 μg ml^{-1} ADR for 2 h, γ-irradiated using a Cs-137 source (Gamma cell-40, Atomic energy of Canada), ultraviolet-irradiated using an ultraviolet cross-linker (XL-1500, Spectronics corporation), or X-irradiated using an X-ray irradiation system (MBR-1520R-3, Hitachi). Mice were also γ-irradiated using a Cs-137 source (Gamma cell-40, Nordion) or X-irradiated using an X-ray irradiation system (MBR-1520R-3, Hitachi).

Quantitative real-time PCR. Peripheral blood mononuclear cells were obtained by separating blood cells in a Ficoll gradient (Amersham). Peripheral blood mononuclear cells were incubated with phytohaemagglutinin for 72 h and exposed to an X-ray irradiation. Total RNA was isolated from mouse tissue or human cells using RNeasy spin column kits (Qiagen) according to the manufacturer's instruction. Blood RNA of irradiated mice was prepared using Mouse RiboPure-Blood RNA Isolation Kit (Ambion). Complementary DNAs were synthesized with the SuperScript Preamplification System (Invitrogen). Quantitative real-time PCR was conducted using the SYBR Green I Master on a LightCycler 480 (Roche). The primer sequences are indicated in Supplementary Table S3.

Immunoprecipitation. Cell extracts from HEK293T cells transfected with plasmids encoding Flag-Lamins and/or HA-PADI4s were prepared by adding HBST buffer (10 mM HEPES at pH 7.4, 150 mM NaCl and 0.5% TritonX-100). Extracts were precleared by incubation with protein G-Sepharose 4B (Zymed) and mouse IgG at 4 °C for 1 h. Precleared cell extracts were then incubated with anti-Flag affinity gel (Sigma) at 4 °C for 2 h. The beads were washed 4 times with 1 ml of ice-cold HBST buffer, and immunoprecipitated proteins were released from the beads by boiling in sample buffer for 2 min.

Western blotting. To prepare whole-cell extracts, cells or tissues were lysed in chilled HBST buffer for 30 min on ice and centrifuged at 16,000*g* for 15 min. Histones were purified in acidic condition as previously described[45]. Samples were subjected to SDS–PAGE and immunoblotting using standard procedures. To detect citrullinated proteins, blots of deiminated proteins were treated with medium for chemical modification at 37 °C for 3 h, and, then, modified citrulline residues were detected with an anti-modified citrulline antibody (anti-MC antibody, Upstate). Bands were quantified by the Image J software.

Table 1 | Association between citrullinated H4R3-positivity and clinicopathological parameters in NSCLC patients.

	Total	cit-H4R3		*P* value
	n=309	Positive	Negative	Positive versus negative
		n=159	*n*=150	
Gender				
Male	214	100	114	0.0138**
Female	95	59	36	
Age (years)				
<65	135	67	68	NS (0.6463)
≧65	174	92	82	
Histological type				
ADC	192	110	82	0.0099**
SCC	82	35	47	
Others	35	14	21	
Smoking status				
Never	90	60	30	0.0007**
Smoker	219	99	120	
pT factor				
T1	132	80	52	0.0136**
T2+T3	177	79	98	
pN factor				
N0	204	104	100	NS (0.9044)
N1+N2	105	55	50	
p53				
Positive	130	55	75	0.0079**
Negative	179	104	75	

Abbreviations: ADC, adenocarcinama; NS, no significance: SCC, squamous-cell carcinoma; Others, large-cell carcinoma plus adenosquamous-cell carcinoma.
**$P<0.05$ (Fisher's exact test).

Antibodies. To develop an antibody against Cit571-572 Lamin C, a Lamin C peptide (LHHHHVSGSCitCit) was chemically synthesized and used to immunize rabbits. The positive antisera were further purified by immune-affinity purification using a Lamin C Cit571-572 peptide. Anti-citrullinated nucleophosmin (NPM) antibody was prepared as previously described[10]. Polyclonal anti-MC antibody (17-347) and anti-citrullinated arginine 3 of histone H4 antibody (07-596) were purchased from Upstate. Anti-β-actin monoclonal antibody (A5441) and Anti-Flag monoclonal (F3165) and polyclonal (F7425) antibodies were purchased from Sigma. Anti-p53 monoclonal antibody (OP140) and anti-Lamin B antibody (NA12) were purchased from Calbiochem. Anti-HA monoclonal (sc-7392) and polyclonal (sc-805) antibodies were purchased from Santa Cruz Biotechnology. Anti-HA rat monoclonal antibody (3F10) was purchased from Roche. Anti-6×His monoclonal antibody (631212) was purchased from Clontech. Anti-PADI4 polyclonal antibody (ab50332), anti-citrullinated histone H3 antibody (ab5103) and anti-mono methyl histone H4 antibody (ab17339) were purchased from Abcam. Anti-Lamin A/C antibody (#2032 or #4777), anti-caspase-3 antibody (#9662) and anti-cleaved caspase-3 (#9661) were purchased from Cell signaling. List of antibodies and the concentrations used are shown in Supplementary Table S4.

***In vitro* citrullination assay**. Recombinant histone proteins were purchased from Millipore. Glutathione *S*-transferase (GST) fusion PADI4 and NPM1 proteins were generated as previously described[10]. His-tagged proteins were generated by cloning of their coding sequences into pET21a or pET28a vector (Novagen). Proteins were expressed in *Escherichia coli* and purified on Ni-NTA agarose (Qiagen) by standard methods. Deimination reactions were carried out as previously described[10].

GST pull-down assay. Core histones were purified from HEK293T cells using Histone Purification Kit (Active motif). GST-NPM (1 μg) and core histones (1 μg) were separately incubated with PADI4 (1 μg) or PADI4-D350A (1 μg) for 1 h at 37 °C with 1 mM of CaCl2. PADI4-treated NPM1 and histones were mixed and stored on ice for 1 h. The mixture was incubated at 4 °C for 2 h with 20 μl of a glutathione–Sepharose 4B bead suspension (Amersham Pharmacia). After the beads were washed extensively, proteins were eluted from the beads by incubation with SDS sample buffer, separated by SDS–PAGE, and visualized by silver staining.

Immunocytochemistry. Immunocytochemistry was performed as previously described[10]. Before incubating with anti-MC antibody, cells were treated with medium for chemically modifying citrulline residues at 37 °C for 3 h. For co-staining of TUNEL and citrullinated proteins, cells were immunostained followed by TUNEL reaction for 1 h at 37 °C using the kit (In Situ Cell Death Detection Kit, Fluorescein, Roche). Quantification was performed by counting around 100 cells from more than 4 independent fields.

Immunohistochemistry. Frozen sections of mouse thymus were used for immunohistochemistry and TUNEL staining. Immunohistochemistry was performed using the immunohistochemistry EnVision (Dako) method. TUNEL staining was performed using Apoptosis in situ Detection Kit (Wako) according to the manufacturer's instruction. Tissue microarrays were constructed in our laboratory, and staining and statistical analysis were performed as previously described[46].

Mutation analysis. Genomic DNA was purified from 80 cancer cell lines by standard protocol[8]. The list of cell lines is shown in Supplementary Table S1. 16 coding exons of the *PADI4* gene were amplified, purified and sequenced. The sequences of primers used in this analysis are indicated in Supplementary Table S3.

Chromatin fractionation. S1, S2 and P chromatin fractions from HEK293T cell nuclei were prepared according to previously described procedures[47] with minor modifications. HEK293T cells were transfected with PADI4-expressing plasmid. The collected cells were incubated in cell homogenization buffer (10 mM Tris at pH 8.0, 10 mM $MgCl_2$, 0.5% NP40 and 1 mM DTT) on ice for 10 min. The nuclear pellet was obtained by centrifugation and resuspended in MNase digestion buffer (15 mM Tris pH 7.4, 15 mM NaCl, 60 mM KCl, 0.25 M sucrose, 1 mM $CaCl_2$). The pellet was then treated with MNase (New England Biolabs) for 2 min at 37 °C. The solution was centrifuged to obtain the supernatant (S1). The pellet was resuspended in 0.1 mM EDTA, incubated at 4 °C for 30 min, and centrifugated to obtain the chromatin fraction (P) and supernatant (S2). The proteins contained in each fraction were separated by 15% SDS–PAGE and detected by western blotting.

MNase assay. The nuclear pellet (Input) was treated with MNase as shown above. The reaction was terminated by adding the stop solution (0.5 mM EGTA, 25 mM EDTA). After centrifugation at 14,000*g* for 5 min, DNA was extracted from the aqueous phase and analysed on agarose gel. Histone proteins collected from the aqueous phase (Sup) and pellet (Ppt) were separated by SDS–PAGE.

Cell death assay. Cells were infected with 20 multiplicity of infection (MOI) of Ad-p53 at 7 h after transfection of siRNA oligonucleotide. 60 h after infection cells were incubated with TUNEL reaction mixture for 1 h at 37 °C using the kit (In Situ Cell Death Detection Kit, Fluorescein, Roche). Apoptotic cells were quantified by fluorescence-activated cell sorting analysis.

References

1. Levine, A. J., Hu, W. & Feng, Z. The P53 pathway: what questions remain to be explored? *Cell Death and Differ.* **13,** 1027–1036 (2006).
2. Vogelstein, B., Lane, D. & Levine, A. J. Surfing the p53 network. *Nature* **408,** 307–310 (2000).
3. Lane, D. P. Cancer. p53, guardian of the genome. *Nature* **358,** 15–16 (1992).
4. Nakamura, Y. Isolation of p53-target genes and their functional analysis. *Cancer Sci.* **95,** 7–11 (2004).
5. Oda, K. *et al.* p53AIP1, a potential mediator of p53-dependent apoptosis, and its regulation by Ser-46-phosphorylated p53. *Cell* **102,** 849–862 (2000).
6. Tanaka, H. *et al.* A ribonucleotide reductase gene involved in a p53-dependent cell-cycle checkpoint for DNA damage. *Nature* **404,** 42–49 (2000).
7. Tanikawa, C., Matsuda, K., Fukuda, S., Nakamura, Y. & Arakawa, H. p53RDL1 regulates p53-dependent apoptosis. *Nat. Cell Biol.* **5,** 216–223 (2003).
8. Tanikawa, C. *et al.* XEDAR as a putative colorectal tumor suppressor that mediates p53-regulated anoikis pathway. *Oncogene* **28,** 3081–3092 (2009).
9. Tanikawa, C., Ri, C., Kumar, V., Nakamura, Y. & Matsuda, K. Crosstalk of EDA-A2/XEDAR in the p53 signaling pathway. *Mol. Cancer Res.* **8,** 855–863 (2010).
10. Tanikawa, C. *et al.* Regulation of protein citrullination through p53/PAD14 network in DNA damage response. *Cancer Res.* **69,** 8761–8769 (2009).
11. Nakashima, K., Hagiwara, T. & Yamada, M. Nuclear localization of peptidylarginine deiminase V and histone deimination in granulocytes. *J. Biol. Chem.* **277,** 49562–49568 (2002).
12. Neeli, I., Khan, S. N. & Radic, M. Histone deimination as a response to inflammatory stimuli in neutrophils. *J. Immunol.* **180,** 1895–1902 (2008).
13. Wang, Y. *et al.* Histone hypercitrullination mediates chromatin decondensation and neutrophil extracellular trap formation. *J. Cell Biol.* **184,** 205–213 (2009).
14. de Seze, J. *et al.* IgG reactivity against citrullinated myelin basic protein in multiple sclerosis. *J. Neuroimmunol.* **117,** 149–155 (2001).
15. Schellekens, G. A. *et al.* The diagnostic properties of rheumatoid arthritis antibodies recognizing a cyclic citrullinated peptide. *Arthritis Rheum.* **43,** 155–163 (2000).
16. Goldbach-Mansky, R. *et al.* Rheumatoid arthritis associated autoantibodies in patients with synovitis of recent onset. *Arthritis Res.* **2,** 236–243 (2000).

17. van Boekel, M. A., Vossenaar, E. R., van den Hoogen, F. H. & van Venrooij, W. J. Autoantibody systems in rheumatoid arthritis: specificity, sensitivity and diagnostic value. *Arthritis Res.* **4,** 87–93 (2002).
18. Suzuki, A. *et al.* Functional haplotypes of PADI4, encoding citrullinating enzyme peptidylarginine deiminase 4, are associated with rheumatoid arthritis. *Nat. Genet.* **34,** 395–402 (2003).
19. Wang, Y. *et al.* Human PAD4 regulates histone arginine methylation levels via demethylimination. *Science* **306,** 279–283 (2004).
20. Cuthbert, G. L. *et al.* Histone deimination antagonizes arginine methylation. *Cell* **118,** 545–553 (2004).
21. Martic, G. *et al.* Parathymosin affects the binding of linker histone H1 to nucleosomes and remodels chromatin structure. *J. Biol. Chem.* **280,** 16143–16150 (2005).
22. Li, P. *et al.* PAD4 is essential for antibacterial innate immunity mediated by neutrophil extracellular traps. *J. Exp. Med.* **207,** 1853–1862 (2010).
23. Arita, K. *et al.* Structural basis for Ca(2+)-induced activation of human PAD4. *Nat. Struct. Mol. Biol.* **11,** 777–783 (2004).
24. Top, B. *et al.* Comparative analysis of p53 gene mutations and protein accumulation in human non-small-cell lung cancer. *Int. J. Cancer* **64,** 83–91 (1995).
25. Bodner, S. M. *et al.* Expression of mutant p53 proteins in lung cancer correlates with the class of p53 gene mutation. *Oncogene* **7,** 743–749 (1992).
26. Jones, P. A. & Baylin, S. B. The epigenomics of cancer. *Cell* **128,** 683–692 (2007).
27. Hollstein, M. *et al.* Database of p53 gene somatic mutations in human tumors and cell lines. *Nucleic Acids Res.* **22,** 3551–3555 (1994).
28. Soussi, T. *et al.* Meta-analysis of the p53 mutation database for mutant p53 biological activity reveals a methodologic bias in mutation detection. *Clin. Cancer Res.* **12,** 62–69 (2006).
29. Beroud, C. & Soussi, T. The UMD-p53 database: new mutations and analysis tools. *Hum. Mutat.* **21,** 176–181 (2003).
30. Jenuwein, T. & Allis, C. D. Translating the histone code. *Science* **293,** 1074–80 (2001).
31. Celeste, A. *et al.* H2AX haploinsufficiency modifies genomic stability and tumor susceptibility. *Cell* **114,** 371–383 (2003).
32. Bassing, C. H. *et al.* Histone H2AX: a dosage-dependent suppressor of oncogenic translocations and tumors. *Cell* **114,** 359–370 (2003).
33. Cheung, W. L. *et al.* Apoptotic phosphorylation of histone H2B is mediated by mammalian sterile twenty kinase. *Cell* **113,** 507–517 (2003).
34. Kouzarides, T. Chromatin modifications and their function. *Cell* **128,** 693–705 (2007).
35. Gyorgy, B., Toth, E., Tarcsa, E., Falus, A. & Buzas, E. I. Citrullination: a posttranslational modification in health and disease. *Int. J. Biochem. Cell Biol.* **38,** 1662–1677 (2006).
36. Li, P. *et al.* Regulation of p53 target gene expression by peptidylarginine deiminase 4. *Mol. Cell. Biol.* **28,** 4745–4758 (2008).
37. Chang, X. *et al.* Increased PADI4 expression in blood and tissues of patients with malignant tumors. *BMC Cancer* **9,** 40 (2009).
38. Brown, N. S. & Bicknell, R. Hypoxia and oxidative stress in breast cancer. Oxidative stress: its effects on the growth, metastatic potential and response to therapy of breast cancer. *Breast Cancer Res.* **3,** 323–327 (2001).
39. Toyokuni, S., Okamoto, K., Yodoi, J. & Hiai, H. Persistent oxidative stress in cancer. *FEBS Lett.* **358,** 1–3 (1995).
40. Arita, K. *et al.* Structural basis for histone N-terminal recognition by human peptidylarginine deiminase 4. *Proc. Natl Acad. Sci. USA* **103,** 5291–5296 (2006).
41. Allfrey, V. G. Structural modifications of histones and their possible role in the regulation of ribonucleic acid synthesis. *Proc. Can. Cancer Conf.* **6,** 313–335 (1966).
42. Denis, H. *et al.* Functional connection between deimination and deacetylation of histones. *Mol. Cell Biol.* **29,** 4982–4993 (2009).
43. Li, P. *et al.* Coordination of PAD4 and HDAC2 in the regulation of p53-target gene expression. *Oncogene* **29,** 3153–3162 (2010).
44. Tsukada, T. *et al.* Enhanced proliferative potential in culture of cells from p53-deficient mice. *Oncogene* **8,** 3313–3322 (1993).
45. Shechter, D., Dormann, H. L., Allis, C. D. & Hake, S. B. Extraction, purification and analysis of histones. *Nat. Protoc.* **2,** 1445–1457 (2007).
46. Kato, T. *et al.* Activation of placenta-specific transcription factor distal-less homeobox 5 predicts clinical outcome in primary lung cancer patients. *Clin. Cancer Res.* **14,** 2363–2370 (2008).
47. Kashiwagi, K., Nimura, K., Ura, K. & Kaneda, Y. DNA methyltransferase 3b preferentially associates with condensed chromatin. *Nucleic Acids Res.* **39,** 874–888 (2011).

Acknowledgements

We thank H. Fujiwara for technical assistance. We thank Dr Nobuaki Yoshida and Dr. Toyomasa Katagiri for helpful discussion. This work was supported partially by grant from Japan Society for the Promotion of Science and Ministry of Education, Culture, Sports, Science and Technology of Japan to K.M. and C.T.; grant from Shiseido to C.T.; and Grant-in-Aid from the Tokyo Biochemical Research Foundation to K.M.

Author contributions

C.T., Y.N. and K.M. conceived the project and planned experiments and analyses, which were performed by C.T., M.E. conducted the mutation analysis. K.U. conducted mass analysis. A.S. and K.Y. provided the *Padi4*$^{-/-}$ mice. K.Mas., E.T. and Y.D. conducted tissue microarray analysis. C.T. summarized the whole results. C.T., K.M. and Y.N. wrote the manuscript.

Additional information

Supplementary Information accompanies this paper at http://www.nature.com/naturecommunications

Competing financial interests: The authors declare no competing financial interests.

Reprints and permission information is available online at http://npg.nature.com/reprintsandpermissions/

How to cite this article: Tanikawa, C. *et al.* Regulation of histone modification and chromatin structure by the p53–PADI4 pathway. *Nat. Commun.* 3:676 doi: 10.1038/ncomms1676 (2012).

nature COMMUNICATIONS

DOI: 10.1038/ncomms3638

Corrigendum: Regulation of histone modification and chromatin structure by the p53–PADI4 pathway

Chizu Tanikawa, Martha Espinosa, Akari Suzuki, Ken Masuda, Kazuhiko Yamamoto, Eiju Tsuchiya, Koji Ueda, Yataro Daigo, Yusuke Nakamura & Koichi Matsuda

Nature Communications 3:676 doi: 10.1038/ncomms1676 (2012); Published 14 Feb 2012; Updated 16 Oct 2013

When preparing Fig. 6 for this Article, the labels 'Padi4 $^{+/+}$' and 'Padi4 $^{-/-}$' at the foot of the histograms in panels b, c and d were accidentally placed under the wrong bars. The correct version of Fig. 6 appears below.

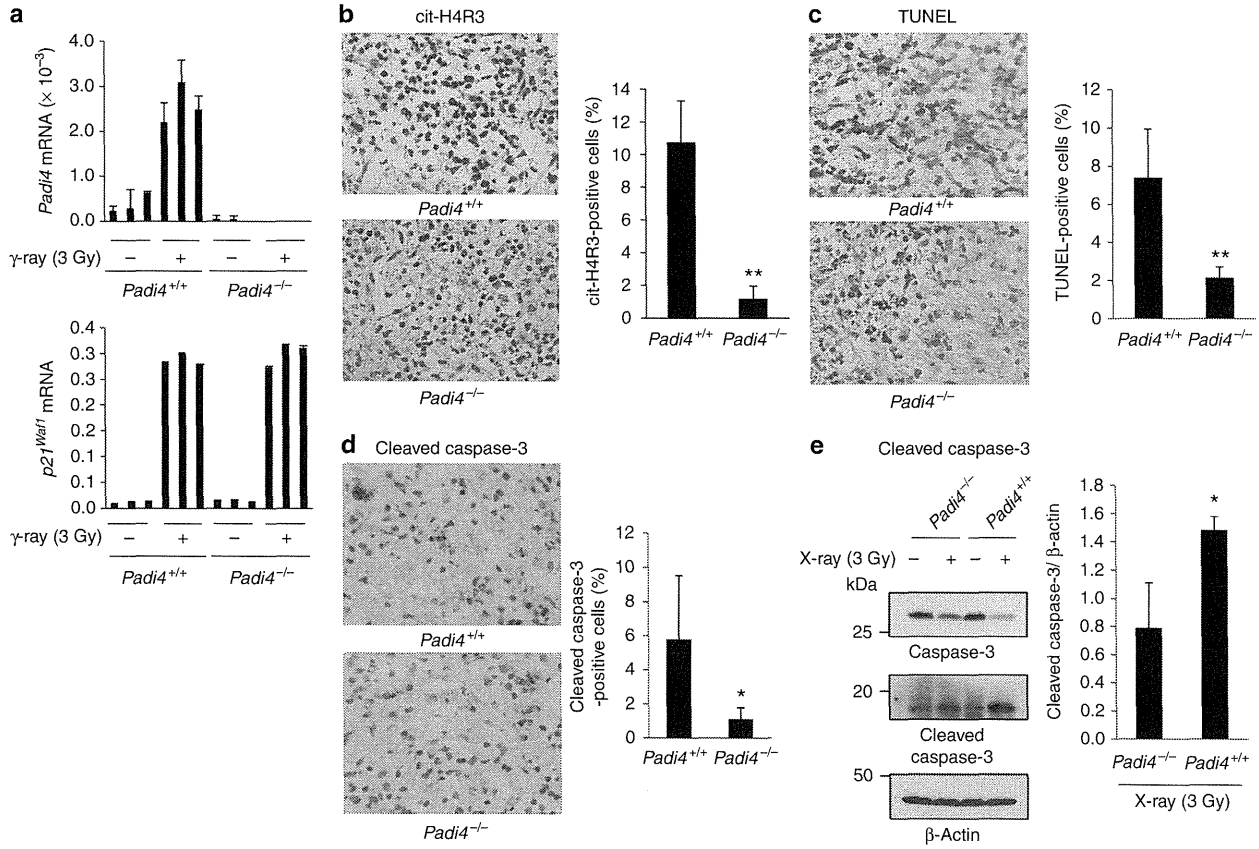

Figure 6

Published OnlineFirst May 3, 2012; DOI: 10.1158/0008-5472.CAN-11-3701

Cancer Research

Histone Lysine Methyltransferase SETD8 Promotes Carcinogenesis by Deregulating PCNA Expression

Masashi Takawa, Hyun-Soo Cho, Shinya Hayami, et al.

Cancer Res 2012;72:3217-3227. Published OnlineFirst May 3, 2012.

Published OnlineFirst May 3, 2012; DOI: 10.1158/0008-5472.CAN-11-3701

Molecular and Cellular Pathobiology

Cancer Research

Histone Lysine Methyltransferase SETD8 Promotes Carcinogenesis by Deregulating PCNA Expression

Masashi Takawa[1,3], Hyun-Soo Cho[1], Shinya Hayami[1], Gouji Toyokawa[1], Masaharu Kogure[1,3], Yuka Yamane[1], Yukiko Iwai[1], Kazuhiro Maejima[1], Koji Ueda[2], Akiko Masuda[5], Naoshi Dohmae[5], Helen I. Field[7], Tatsuhiko Tsunoda[6], Takaaki Kobayashi[3], Takayuki Akasu[4], Masanori Sugiyama[3], Shin-ichi Ohnuma[9], Yutaka Atomi[3], Bruce A.J. Ponder[8], Yusuke Nakamura[1,10], and Ryuji Hamamoto[1,8]

Abstract

Although the physiologic significance of lysine methylation of histones is well known, whether lysine methylation plays a role in the regulation of nonhistone proteins has not yet been examined. The histone lysine methyltransferase SETD8 is overexpressed in various types of cancer and seems to play a crucial role in S-phase progression. Here, we show that SETD8 regulates the function of proliferating cell nuclear antigen (PCNA) protein through lysine methylation. We found that SETD8 methylated PCNA on lysine 248, and either depletion of SETD8 or substitution of lysine 248 destabilized PCNA expression. Mechanistically, lysine methylation significantly enhanced the interaction between PCNA and the flap endonuclease FEN1. Loss of PCNA methylation retarded the maturation of Okazaki fragments, slowed DNA replication, and induced DNA damage, and cells expressing a methylation-inactive PCNA mutant were more susceptible to DNA damage. An increase of methylated PCNA was found in cancer cells, and the expression levels of SETD8 and PCNA were correlated in cancer tissue samples. Together, our findings reveal a function for lysine methylation on a nonhistone protein and suggest that aberrant lysine methylation of PCNA may play a role in human carcinogenesis. *Cancer Res; 72(13); 3217–27. ©2012 AACR.*

Introduction

Protein methylation is recently considered an important posttranslational modification and is predominantly found on lysine and arginine residues. Lysine methylation involves the addition of 1 to 3 methyl groups on the amino acid's ε-amine group, to form mono-, di-, or tri-methyllysine. Its function is best understood in histones (1). With the exception of Dot1/DOT1L, all histone lysine methyltransferases (HKMT) contain a SET domain of about 130 amino acids, and so far nearly 40 SET domain–containing HKMTs or potential HKMTs have been identified (2). While our knowledge of the physiologic functions of HKMTs is growing, their involvement in human diseases including cancer is still not well understood.

Proliferating cell nuclear antigen (PCNA) is an evolutionally well-conserved protein found in all eukaryotic species from yeast to humans, as well as in archaea. PCNA functions are related to vital cellular processes such as DNA replication, chromatin remodeling, DNA repair, sister chromatid cohesion, and cell-cycle control (3). PCNA was originally reported as an antigen for autoimmune disease in patients with systemic lupus erythematosus, detected only in the proliferating cell populations (4). Thereafter, it was shown that expression levels of PCNA during cell cycle are differential and associated with proliferation and transformation (5, 6). In the following years, a number of experiments have been done to uncover the role of PCNA in DNA replication, and one of the first functions clarified was a sliding clamp for DNA polymerase δ (7, 8). Meanwhile, the progress in the field not only strengthened the importance of PCNA, but also even placed PCNA at the crossroad of many essential pathways. Importantly, PCNA is posttranslationally modified in several ways, which affects its function. So far, it has been reported that PCNA is ubiquitinated, phosphorylated, acetylated, and even SUMOylated (3). One of the well-documented posttranslational modifications of PCNA is ubiquitination. In response to DNA damage, PCNA is monoubiquitinated at the lysine 164 residue by the E2 Ub–conjugated enzyme Rad6 and the E3 Ub ligase Rad18 (Rad6/Rad18 complex; ref. 9). Rad18 not only binds to Rad6 and PCNA, but also to DNA (10). Thus, Rad18 recruits the ubiquitination machinery to the chromatin-bound target, PCNA. In addition

Authors' Affiliations: [1]Laboratory of Molecular Medicine, Human Genome Center, Institute of Medical Science, The University of Tokyo; [2]Laboratory for Biomarker Development, RIKEN, Minato-ku; [3]Department of Surgery, Kyorin University School of Medicine, Mitaka; [4]Division of Colorectal Surgery, National Cancer Center Hospital, Chuo-ku, Tokyo; [5]Biomolecular Characterization Team, RIKEN, Wako, Saitama; [6]Laboratory for Medical Informatics, RIKEN, Yokohama, Kanagawa, Japan; Departments of [7]Genetics and [8]Oncology, Cancer Research UK, Cambridge Research Institute, University of Cambridge, Cambridge; [9]Institute of Ophthalmology, University College London, London, United Kingdom; and [10]Section of Hematology/Oncology, The University of Chicago, Chicago, Illinois

Note: Supplementary data for this article are available at Cancer Research Online (http://cancerres.aacrjournals.org/).

M. Takawa and H.-S. Cho contributed equally to this work.

Corresponding Author: Ryuji Hamamoto, Laboratory of Molecular Medicine, Human Genome Center, Institute of Medical Science, The University of Tokyo, 4-6-1 Shirokanedai, Minato-ku, Tokyo 108-8639, Japan. Phone: 81-3-5449-5233; Fax: 81-3-5449-5123; E-mail: ryuji@ims.u-tokyo.ac.jp

doi: 10.1158/0008-5472.CAN-11-3701

Published OnlineFirst May 3, 2012; DOI: 10.1158/0008-5472.CAN-11-3701

to ubiquitination, it is estimated that approximately 6% of chromatin-bound PCNA is subjected to phosphorylation on Tyr 211 (11). It has been considered that phosphorylation of Tyr 211 on PCNA may stabilize chromatin-bound PCNA, as opposed to polyubiquitination. Furthermore, acetylation is another modification detected on PCNA (12), and in yeast, a poly-SUMOylation on PCNA has been described (13). However, functions of lysine methylation on PCNA have never been elucidated.

In this study, we showed that the histone methyltransferase SETD8 methylates Lys 248 on PCNA and regulates functions of PCNA in cancer cells. This is the first report to describe the significance of lysine methylation on PCNA.

Materials and Methods

Cell line

MRC-5, CCD-18Co, 5637, SW780, SCaBER, UMUC3, RT4, T24, HT-1376, A549, H2170, HCT116, LoVo, and 293T cells were from American Type Culture Collection in 2001 and 2003 and tested and authenticated by DNA profiling for polymorphic short tandem repeat (STR) markers, except for SW780. The SW780 line was established in 1974 by A. Leibovitz from a grade I transitional cell carcinoma. RERF-LC-AI and SBC5 cells were from Japanese Collection of Research Bioresources (JCRB) in 2001, and tested and authenticated by DNA profiling for polymorphic short tandem repeat (STR) markers. 253J and 253J-BV cells were from Korean Cell Line Bank (KCLB) in 2001, and tested and authenticated by DNA profiling for polymorphic STR markers. EJ28 cells were from Cell Line Service (CLS) in 2003, and tested and authenticated by DNA profiling for polymorphic STR markers. ACC-LC-319 cells were from Aichi Cancer Center in 2003, and tested and authenticated by DNA profiling for single-nucleotide polymorphism, mutation, and deletion analysis.

Tissue samples and RNA preparation

Bladder tissue samples and RNA preparation were described previously (14–17). Uroplakin is a marker of urothelial differentiation and is preserved in up to 90% of epithelially derived tumors (18). Use of tissues for this study was approved by Cambridgeshire Local Research Ethics Committee (Ref 03/018).

Quantitative real-time PCR

Specific primers for all human *GAPDH* (glyceraldehyde-3-phosphate dehydrogenase; housekeeping gene), *SDH* (housekeeping gene), *SETD8*, and *PCNA* were designed (primer sequences in Supplementary Table S1). PCR reactions were conducted with the LightCycler 480 System (Roche Applied Science) following the manufacturer's protocol.

siRNA transfection

siRNA oligonucleotide duplexes were purchased from Sigma-Genosys for targeting the human *SETD8* transcript. siEGFP, siFFLuc, and siNegative control (siNC), which is a mixture of 3 different oligonucleotide duplexes, were used as control siRNAs. The siRNA sequences are described in Supplementary Table S2. siRNA duplexes (100 nmol/L final concentration) were transfected into bladder and lung cancer cell lines with Lipofectamine 2000 (Life Technologies) for 72 hours, and cell viability was examined by Cell Counting Kit-8 (Dojindo).

Results

SETD8 is overexpressed in various types of cancer and regulates the growth of cancer cells

To investigate roles of a HKMT in human carcinogenesis, we had examined expression levels of several HKMTs in a small subset of clinical bladder cancer samples and found a significant difference in expression levels of *SETD8* between normal and cancer cells (data not shown). We then analyzed 124 bladder cancer samples and 28 normal control samples and confirmed the significant elevation of *SETD8* expression in tumor cells compared with normal cells (Supplementary Table S4). Expression levels partly correlated with the grade of malignancy in bladder cancer (Supplementary Fig. S1A). We also found overexpression of *SETD8* in both non–small cell lung carcinoma (NSCLC) and small cell lung carcinoma (SCLC; Fig. 1A). Subsequent immunohistochemical analysis using anti-SETD8 antibody identified strong SETD8 staining mainly in the nuclei of malignant cells, but no staining in nonneoplastic tissues (Fig. 1B). In addition, our expression profiling analysis indicated the upregulation of *SETD8* in chronic myelogenous leukemia, hepatocellular carcinoma, and pancreatic cancer (Supplementary Fig. S2 and Table S5). Furthermore, a high level of *SETD8* was identified in various cancer cell lines than in a normal lung cell line SAEC (Supplementary Fig. S3).

To investigate the role of SETD8 in the growth of cancer cells, we conducted a knockdown experiment using 2 independent siRNAs against SETD8 (siSETD8#1 and #2) and 2 control siRNAs (siEGFP and siFFLuc). We transfected each of these siRNAs into SW780 bladder cancer cells and found that SETD8 expression was efficiently suppressed by either of the 2 different siRNAs targeting SETD8, compared with control siRNAs (Supplementary Fig. S1B). Using the same siRNAs, we conducted cell growth assays and found significant growth-suppressive effects on 1 bladder cell line (SW780) and 2 lung cancer cell lines (RERF-LC-AI and SBC5), whereas no effect was observed when we used control siRNAs (Fig. 1C). Detailed cell-cycle analysis using flow cytometry indicated that the cell populations of cancer cells lacking SETD8 had a significant increase in the amount of S-phase and sub-G_1 phase cells and a concomitant reduction in the proportion of G_1 cells (Fig. 1D). Furthermore, we showed that in bromodeoxyuridine (BrdUrd) incorporation analysis, the amount of newly incorporated BrdUrd in cancer cells was significantly decreased after treatment with siSETD8 (Fig. 1E), implying that knockdown of SETD8 results in the retardation of DNA replication in cancer cells. These results indicated that SETD8 might play an important role in the regulation of cancer cell growth, especially in S-phase, and knockdown of SETD8 would cause apoptosis of cancer cells.

Published OnlineFirst May 3, 2012; DOI: 10.1158/0008-5472.CAN-11-3701

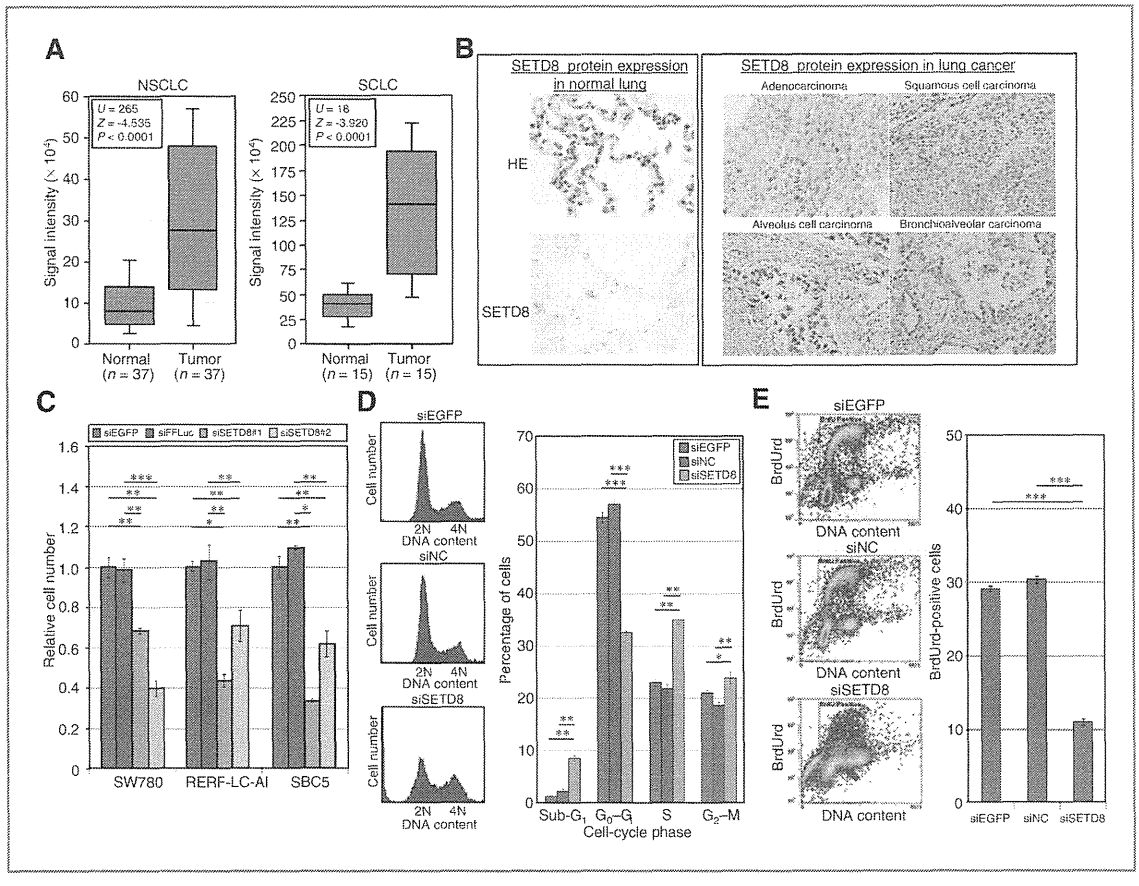

Figure 1. SETD8 is overexpressed in human cancer and regulates the proliferation of cancer cells. A, expression of *SETD8* is significantly increased in tumor tissues compared with normal Japanese patients. Signal intensity for each sample was analyzed by cDNA microarray. B, immunohistochemical staining of SETD8 in lung tissues. Clinical information for each section is represented above histologic pictures. Original magnification, × 100. HE, hematoxylin and eosin. C, effects of *SETD8* siRNA knockdown on the viability of bladder (SW780) and lung (RERF-LC-AI and SBC5) cancer cell lines. Relative cell numbers were normalized to the number of siEGFP-treated cells (siEGFP = 1): results are the mean ± SD of 3 independent experiments. *P* values were calculated using Student *t* test (*, $P < 0.05$; **, $P < 0.01$; ***, $P < 0.001$). D, effect of SETD8 knockdown on cell-cycle kinetics in cancer cells. Cell-cycle distribution was analyzed by flow cytometry after staining with propidium iodide (PI). Left, representative histograms of SBC5 cells stained with PI. Right, numerical analysis of fluorescence-activated cell-sorting (FACS) results in SBC5 cells, classifying cells by cell-cycle status. Results are the mean ± SD of 3 independent experiments. *P* values were calculated using Student *t* test (**, $P < 0.01$; ***, $P < 0.001$). E, detailed cell-cycle kinetics in SBC5 cells after treatment with siSETD8. Cell-cycle distribution was analyzed by flow cytometry after coupled staining with fluorescein isothiocyanate (FITC)-conjugated anti-BrdUrd and 7-amino-actinomycin D (7-AAD) as described in Materials and Methods.

SETD8 methylates lysine 248 of PCNA both *in vitro* and *in vivo*

As PCNA is known to be a key regulator of cell-cycle progression and SETD8 is a component of the PCNA complex (19, 20), we examined the functional relationship between SETD8 and PCNA. Immunoprecipitation assay showed that 3xFLAG-tagged SETD8 bound endogenous PCNA (Fig. 2A). We also confirmed the interaction between endogenous PCNA and SETD8 proteins (Fig. 2B); endogenous SETD8 and PCNA proteins were colocalized in HeLa cells (Fig. 2C). Immunoprecipitation using deletion mutants of SETD8 showed that its N-terminal region of SETD8 is essential for binding to PCNA (Fig. 2D), and this portion contains a PCNA-interacting protein (PIP) box (Supplementary Fig. S4A). Because histone methyltransferases have been found to methylate nonhistone substrates, we evaluated a possibility of PCNA to be a substrate of SETD8. First, we conducted an *in vitro* methyltransferase assay and confirmed that PCNA was methylated in a dose-dependent manner (Fig. 2E). The amino acid analysis detected a single lysine methylation site in PCNA following this reaction (Supplementary Fig. S5). To verify *in vivo* SETD8-dependent PCNA methylation, we labeled 293T cells after transfection with FLAG-PCNA (WT) and hemagglutinin (HA)-mock or HA-SETD8 (1-352) expression vectors with L-[methyl-^{3}H] methionine and found that SETD8 could methylate PCNA *in vivo* (Supplementary Fig. S6A). Subsequent liquid chromatography/tandem mass spectrometry (LC/MS-MS) analysis identified monomethylation at lysine 248 on PCNA by SETD8 (Fig. 2F). To

Published OnlineFirst May 3, 2012; DOI: 10.1158/0008-5472.CAN-11-3701

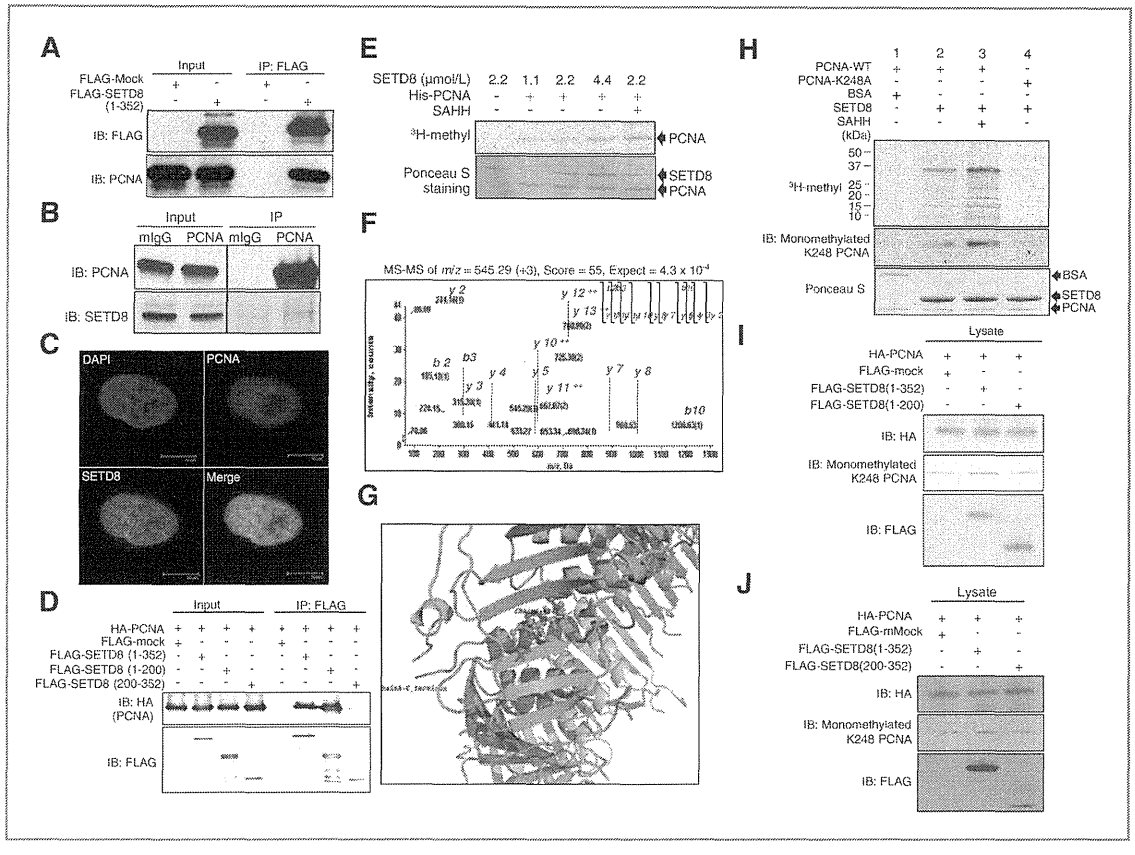

Figure 2. SETD8 methylates lysine 248 of PCNA both *in vitro* and *in vivo*. A, FLAG-mock and FLAG-SETD8 expression vectors were transfected into 293T cells. After 48 hours, cells were immunoprecipitated (IP) with anti-FLAG M2 agarose beads, and immunoprecipitants were immunoblotted (IB) with anti-FLAG (F7425; Sigma-Aldrich) and anti-PCNA (PC10, Santa Cruz Biotechnology) antibodies, respectively. B, SBC5 cells were lysed and immunoprecipitated with normal mouse IgG (mIgG) and anti-PCNA antibody (PC10). The immunoprecipitates were fractionated by SDS-PAGE and blotted with anti-PCNA (PC10) and anti-SETD8 (ab3798, Abcam) antibodies. C, immunocytochemical analysis of HeLa cells. Cells were stained with an anti-PCNA antibody [PC10, Cell Signaling Technology; Alexa Fluor 594 (red)], an anti-SETD8 antibody [C18B7, Cell Signaling Technology; Alexa Fluor 488 (green)], and 4′,6′-diamidine-2′-phenylindole dihydrochloride [DAPI (blue)]. D, 293T cells were transfected with HA-PCNA and FLAG-mock or indicated FLAG-SETD8 expression vectors containing deletion variants. Cell lysates were immunoprecipitated with anti-FLAG M2 agarose beads. Samples were fractionated by SDS-PAGE and blotted with anti-HA (Y-11, Santa Cruz Biotechnology) and anti-FLAG (F7425) antibodies. E, *in vitro* methyltransferase assay of PCNA. Recombinant His-PCNA and ^{3}H-SAM were incubated in the presence or absence of recombinant SETD8, and the reaction products were analyzed by SDS-PAGE followed by fluorography (top). The membrane was stained with Ponceau S (bottom). F, the MS-MS spectrum corresponding to the monomethylated PCNA 241–254 peptide. The 14 Da increase of the Lys 248 residue was observed, showing the monomethylated Lys 248. Score and Expect show Mascot Ion Score and Expectation value in Mascot Database search results, respectively. G, structure of the methylation site in PCNA protein analyzed by PyMOL. H, validation of an anti-monomethylated K248 PCNA antibody. Recombinant PCNA-WT or PCNA-K248A proteins and ^{3}H-SAM were incubated in the presence or absence of recombinant SETD8, and the reaction products were analyzed by SDS-PAGE followed by fluorography (top). The membrane was immunoblotted with an anti-monomethylated K248 antibody (middle) and stained with Ponceau S (bottom). BSA, bovine serum albumin. I and J, 293T cells were cotransfected with an HA-PCNA vector and an empty vector (FLAG-mock), a FLAG-SETD8 (1-352) vector, (1-200, ΔSET) vector, or a FLAG-SETD8 (200-352, ΔPIP box) vector. The samples were immunoblotted with anti-monomethylated K248 PCNA, anti-FLAG, and anti-HA antibodies. SAHH, S-adenosyl-L-homocysteine hydrolase.

validate this result, we constructed the plasmid (PCNA-K248A) that was designed to substitute lysine 248 of PCNA protein to alanine and conducted *in vitro* methyltransferase assay (Supplementary Fig. S6B). The intensity of the band corresponding to PCNA methylation in PCNA-K248A was significantly diminished compared with that of the wild-type PCNA (PCNA-WT). These data show that lysine 248, which is highly conserved in the PCNA ortholog from green alga to human (Supplementary Fig. S4B), is the primary target of SETD8-dependent methylation (Fig. 2G). On the basis of this result, we generated an antibody against a methylated K248 synthetic peptide (Supplementary Fig. S7A) that showed high affinity and high specificity by ELISA (Supplementary Fig. S7B). Western blot analysis using this antibody confirmed that it specifically recognizes K248-methylated PCNA (Fig. 2H and Supplementary Fig. S7C and S7D), and this specific signal was dependent on the methyltransferase activity of SETD8 (Fig. 2I). Importantly, the methyltransferase activity of N-terminal–deleted SETD8 protein, which lacks the PIP box domain, was significantly low than that of wild-type SETD8 protein (Fig. 2J). This

Published OnlineFirst May 3, 2012; DOI: 10.1158/0008-5472.CAN-11-3701

result indicates that the N-terminal region of SETD8 containing PIP box domain seems to be important for SETD8-dependent PCNA methylation. This antibody was used to examine the methylation status of PCNA *in vivo* after treatment with siSETD8 (Supplementary Fig. S8). Monomethylation of PCNA at lysine 248 diminished after knockdown of SETD8 in SBC5 cells, implying SETD8-dependent PCNA K248 methylation occurs both *in vitro* and *in vivo*.

SETD8 stabilizes PCNA protein through the methylation of lysine 248

To clarify the physiologic significance of PCNA methylation by SETD8, we examined protein expression levels of PCNA in SW780 cells 48 hours after knockdown of SETD8 using 2 independent siRNAs (Fig. 3A). Knockdown of SETD8 decreased PCNA protein, suggesting involvement of SETD8 in regulating PCNA stability in cancer cells. To further validate this result, we examined the cell-cycle dependency of SETD8 and PCNA protein expression levels after aphidicolin synchronization (Fig. 3B). Intriguingly, when we treated with SETD8 siRNAs, PCNA protein expression decreased in both G_1 and S-phases according to the levels of SETD8, indicating that SETD8 is likely to be a key regulator of PCNA protein expression at G_1 and S-phases. Because quantitative real-time PCR analysis implied that *PCNA* mRNA level was not affected by treatment with siSETD8 (Fig. 3B), the regulation of PCNA expression by SETD8 was not at the transcriptional level but at the protein level. To examine that this regulation is mediated by SETD8-dependent methylation, we examined PCNA (WT) or PCNA (K248A) protein expression levels in 293T cells transfected with mock

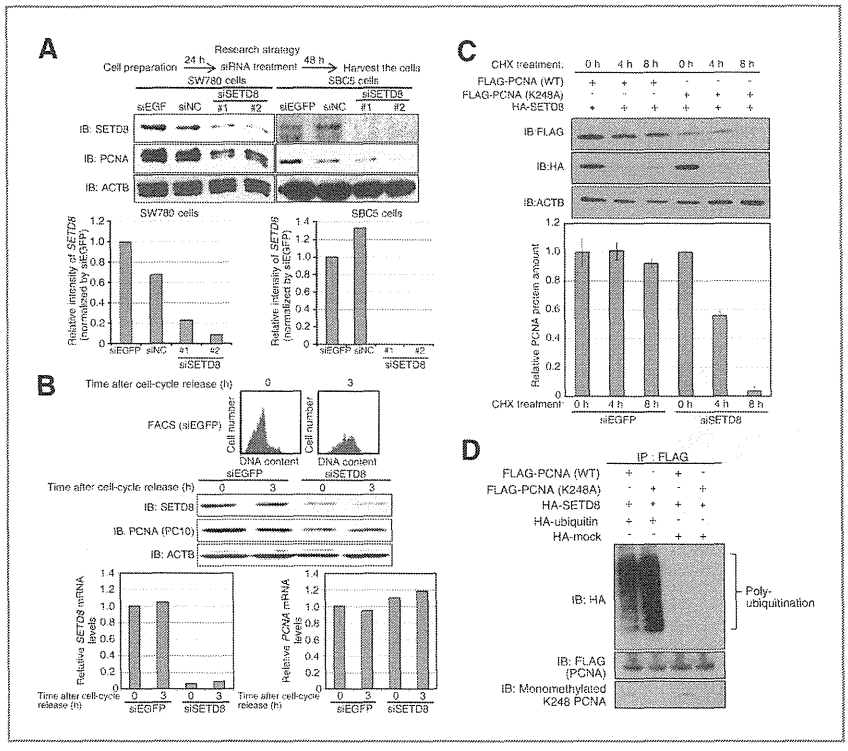

Figure 3. SETD8 stabilizes PCNA protein through the methylation of lysine 248. A, top, validation of SETD8 and PCNA expressions at the protein level. Lysates from SW780 and SBC5 cells, 48 hours after treatment with 2 control siRNAs (siEGFP and siNC) and 2 different siRNAs targeting SETD8 (siSETD8), were immunoblotted (IB) with anti-SETD8 (ab3798), anti-PCNA (PC10), and anti-ACTB (I-19, Santa Cruz Biotechnology) antibodies. β-actin (ACTB) served as an internal control. Bottom, the signal intensity corresponding SETD8 protein was quantified by ImageJ (http://rsb.info.nih.gov/ij/index.html). B, effects of SETD8 knockdown on the stability of PCNA in SW780 cells after synchronizing the cell cycle. SW780 cells were treated with siEGFP and siSETD8#2 for 24 hours and synchronized the cell cycle with 7.5 μg/mL aphidicolin. After 24 hours of treatment, the culture medium was changed, and the cells were collected at 0 and 3 hours after the release from cell-cycle arrest. Cell-cycle status was analyzed by FACS (top, red), and cell lysates were immunoblotted with anti-SETD8 (ab3798), anti-PCNA (PC10), and anti-ACTB (I-19) antibodies (middle). Expression of ACTB was the internal control. Transcriptional expression levels of *SETD8* and *PCNA* were quantified by real-time PCR (bottom). C, SETD8 stabilizes PCNA protein through K248 methylation. 293T cells were transfected with FLAG-PCNA (WT) or FLAG-PCNA (K248A) and HA-SETD8 (1-352) expression vectors. After 24 hours, cells were treated with 100 μg/mL of cycloheximide (CHX) for 4 and 8 hours, then immunoblotted with anti-HA (Y-11), anti-FLAG (F7425), and anti-ACTB (I-19) antibodies. Signal intensities of PCNA and ACTB proteins were quantitatively analyzed by GS-800 (Bio-Rad), and each PCNA intensity was normalized by ACTB intensity. Relative PCNA protein amount shows the intensity value standardized by the intensity at 0 hour (both siEGFP- and siSETD8-treated samples, 0 h = 1): results are the mean ± SD of triplicate experiments. D, ubiquitin assay of exogenous PCNA. FLAG-PCNA (WT) or FLAG-PCNA (K248A) and HA-SETD8 (1-352) expression vectors were transfected into 293T cells together with a HA-ubiquitin or HA-mock expression vector. Cell lysates were immunoprecipitated (IP) with anti-FLAG M2 agarose beads and immunoblotted with anti-FLAG (F7425), anti-HA (Y-11), and anti-monomethylated K248 PCNA antibodies.

Published OnlineFirst May 3, 2012; DOI: 10.1158/0008-5472.CAN-11-3701

or SETD8 expression vectors after cycloheximide treatment. Although wild-type PCNA was significantly stabilized by SETD8 expression, methylation-inactive mutant PCNA (PCNA-K248A) was unstable (Fig. 3C). Furthermore, we examined the PCNA stability in endogenous level after depletion of SETD8 and found that the degradation rate of PCNA in cells treated with siSETD8 more rapidly than siEGFP (Supplementary Fig. S9). Taken together, SETD8-dependent methylation is crucial for PCNA stabilization. Then, we validated the effect of SETD8-dependent methylation on ubiquitination of PCNA proteins. The PCNA (WT) or PCNA (K248A) expression vector was cotransfected into 293T cells with a vector expressing either the full-length or N-terminal region of SETD8, and ubiquitination and methylation status of PCNA was examined (Fig. 3D). As we expected, the status of ubiquitination and methylation on PCNA showed the inverse correlation. Hence, we consider that methylation of PCNA inhibited its ubiquitination. We also examined the phosphorylation status of Tyr 211 on PCNA, which is known to influence the stability of PCNA (11), but no significant relationship between methylation and phosphorylation status was observed (data not shown). These data show that PCNA protein is stabilized through inhibition of the ubiquitination by its SETD8-dependent methylation.

Methylation of lysine 248 on PCNA affects its interaction with FEN1

We conducted immunoprecipitation analysis to further investigate the significance of PCNA methylation, using wild-type and methylation-inactive mutant PCNA proteins, and identified a partner protein, FEN1, which interacted with

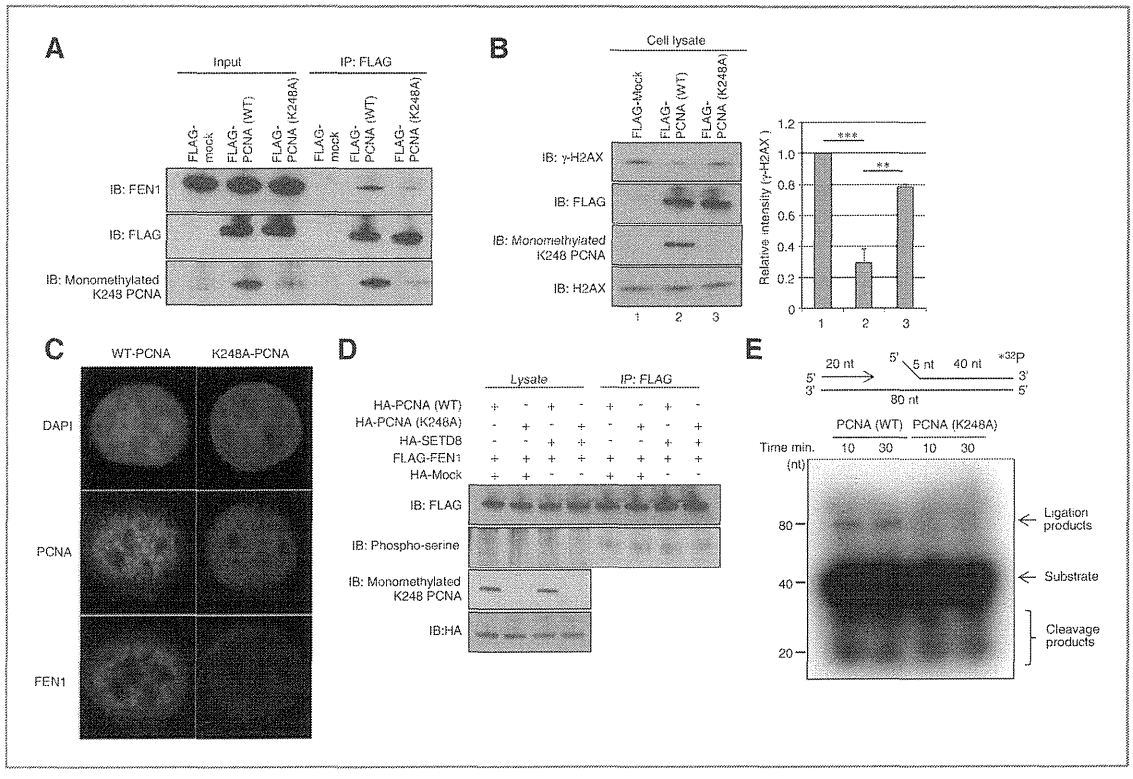

Figure 4. Methylation of PCNA is crucial for the interaction with FEN1. A, K248 monomethylation affected the interaction of PCNA with FEN1. 293T cells were transfected with a FLAG-PCNA (WT) vector or a FLAG-PCNA (K248A) vector together with an HA-SETD8 vector. Immunoprecipitation (IP) was conducted using anti-FLAG M2 agarose and samples were immunoblotted (IB) with anti-FLAG (F7425), anti-FEN1 (HPA006748, Sigma-Genosys), and anti-monomethylated K248 PCNA antibodies. B, double-strand DNA breaks were detected by Western blotting using an anti-γH2AX antibody (05-636, Millipore). Lysates from 293T cells transfected with a FLAG-PCNA (WT) or a FLAG-PCNA (K248A) and were immunoblotted with anti-FLAG (F7425), anti-monomethylated K248 PCNA, anti-γH2AX (05-636), and anti-H2AX (07-627, Millipore) antibodies. Signal intensity was quantified by ImageJ. Results are the mean of 2 independent experiments. C, subcellular localization of PCNA and FEN1 in S-phase. HeLa cells transfected with a FLAG-PCNA (WT) vector or a FLAG-PCNA (K248A) vector were synchronized at late G_1 phase by treatment with mimosine (400 μmol/L for 12 hours). Cell cycle was released by removing mimosine, and cells were costained with anti-FLAG (F7425) and anti-FEN1 (HPA006748) antibodies. Scale bar, 5 μm. D, methylation of PCNA does not alter FEN1 phosphorylation. 293T cells were cotransfected with a HA-PCNA (WT) vector or a HA-PCNA (K248A) together with HA-SETD8 and FLAG-FEN1 expression vectors. Immunoprecipitation was conducted using anti-FLAG M2 agarose, and samples were immunoblotted with anti-FLAG (F7425), anti-HA (Y-11), anti-monomethylated K248 PCNA, and anti-phospho-serine (4A4, Millipore) antibodies. E, Okazaki fragment maturation assay. A schematic diagram of the assay (top) showing a gap substrate (20 mer and 40 mer,top; with an 80-mer complementary strand, bottom) with a 5-nt DNA flap (40 mer, top right strand, with or without a ^{32}P label attached). The gap substrate was incubated with wild-type PCNA [FLAG-PCNA (WT)] and mutant-type PCNA [FLAG-PCNA (K248A)].

Published OnlineFirst May 3, 2012; DOI: 10.1158/0008-5472.CAN-11-3701

PCNA in a methylation-dependent manner. Methylation of PCNA significantly enhanced the interaction between PCNA and FEN1 (Fig. 4A). To validate the effect of PCNA methylation on the interaction with FEN1 in more detail, we conducted an *in vitro* binding assay using methylated PCNA and unmethylated PCNA with FEN1 recombinant protein. SETD8-dependent lysine methylation of PCNA significantly enhanced the interaction between PCNA and FEN1 *in vitro* (Supplementary Fig. S10). FEN1 is a structure-specific nuclease with both 5′ flap endonuclease and 5′-3′ exonuclease activities (21). During DNA replication, this enzyme is responsible for RNA primer removal during Okazaki fragment processing and was identified as the factor responsible for the completion of replication *in vitro* (22). Yeast cells lacking the *FEN1* gene (also called *RAD27*) are viable but are unable to grow at high temperatures, indicating defective DNA replication (23). To examine the effect of PCNA methylation on FEN1 function, we measured levels of the phosphorylated form of H2AX histone variant (γH2AX), an early marker of the cellular response to DNA breaks. In the absence of any exogenous source of DNA damage, basal levels of phosphorylated γH2AX in 293T cells expressing methylation-inactive mutant PCNA (PCNA-K248A) were higher than those in 293T cells expressing wild-type PCNA (Fig. 4B). This implies the accumulation of DNA double-strand breaks resulting from methylation-inactive mutant PCNA expression. During the S-phase of the cell cycle, FEN1 is recruited to DNA replication loci through the interaction with PCNA. Disruption of the FEN1–PCNA interaction impairs such localization (24).

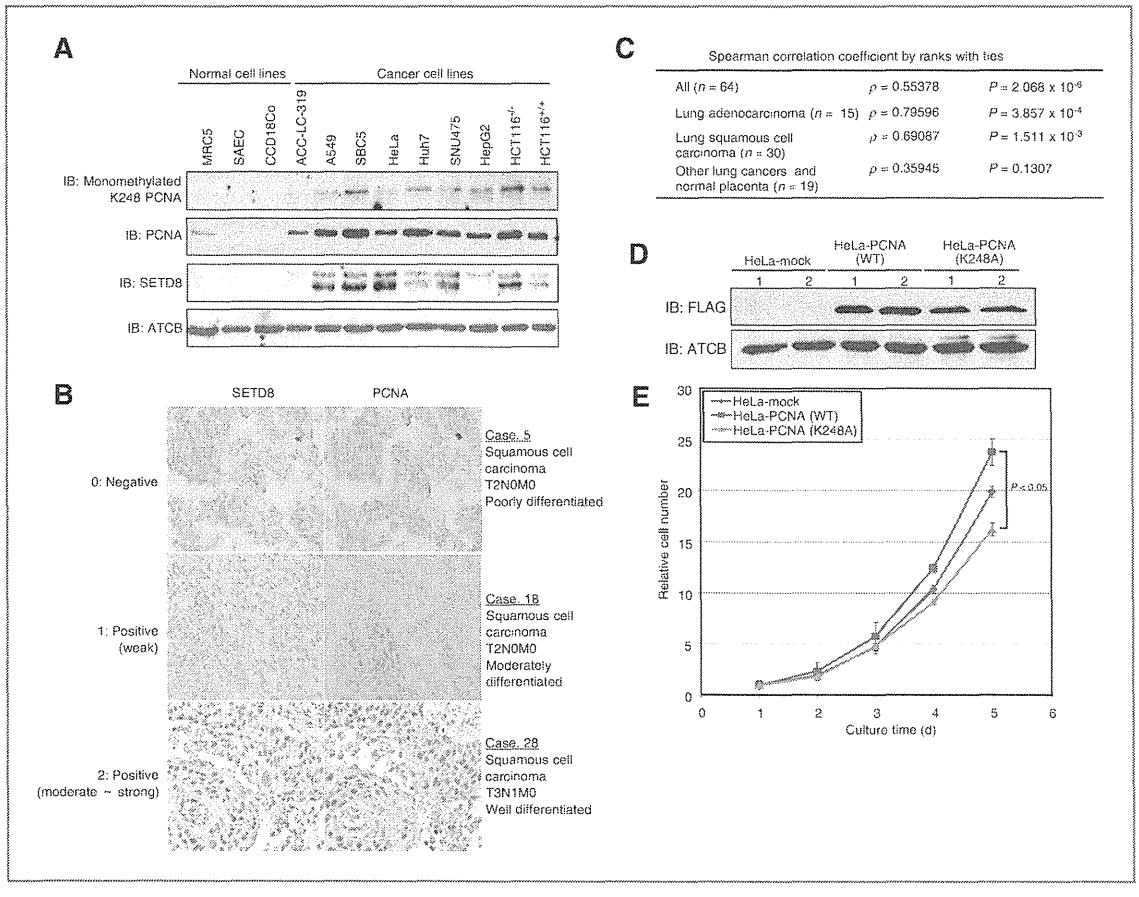

Figure 5. SETD8 and PCNA are coexpressed in lung cancer tissues, and methylation of PCNA promotes the proliferation of cancer cells. A, validation of PCNA methylation status in various cell lines. Lysates from normal cell lines and cancer cell lines were immunoblotted (IB) with anti-monomethylated K248 PCNA and anti-ACTB (I-19) antibodies. B, immunohistochemical stainings of SETD8 and PCNA in lung cancer tissues. Three typical stained case tissues are shown, with staining intensity of each case categorized into 3 patterns: 0 (no staining), 1 (weak staining), and 2 (moderate or strong staining). Detailed clinical information is described in Supplementary Table S6. C, correlation of staining between SETD8 and PCNA was statistically calculated using Spearman correlation coefficient by ranks with ties. D, construction of HeLa stable cell lines overexpressing wild-type PCNA [HeLa-PCNA (WT)] and K248-substituted PCNA [HeLa-PCNA (K248A)]. Empty vector–transfected HeLa stable cell lines were used as a control (HeLa-mock). Lysates from each cell line were immunoblotted with anti-FLAG (F7425) and anti-ACTB (I-19) antibodies. E, the cell growth assay was conducted using HeLa stable cell lines. Number of cells was measured by Cell Counting Kit-8 (Dojindo) and relative cell number shows the value normalized by the number of cells at day 1 (day 1 = 1). Results are the mean ± SD in 3 independent experiments. *P* values were calculated using Student *t* test.

Published OnlineFirst May 3, 2012; DOI: 10.1158/0008-5472.CAN-11-3701

If methylation of PCNA were important for interacting with FEN1, failure in methylation would lead to a defect in FEN1's localization to replication foci. FEN1 could be colocalized with PCNA at replication foci in cells when PCNA was a wild-type. However, FEN1 was unable to localize to the foci in cells in which methylation-inactive mutant was present (Fig. 4C). These data suggest that PCNA methylation is important for regulation of FEN1's subnuclear localization. Because phosphorylation of FEN1 has been shown to abolish its PCNA interaction (25), we examined FEN1 phosphorylation status in cells expressing wild-type and methylation-inactive mutant PCNA, but found no significant difference in phosphorylation status of FEN1 between wild-type and methylation-inactive mutant PCNA–expressing cells (Fig. 4D). This implies that the different affinity between PCNA and FEN1 seems to be regulated not by phosphorylation status of FEN1 but by methylation status of PCNA (as shown in Fig. 4A and C). Furthermore, an Okazaki fragment maturation assay was conducted using the deoxynucleotide triphosphate mixture containing radiolabeled dCTP and a model substrate containing an RNA-DNA flap, which mimicked the Okazaki fragment maturation intermediate. The assay simulates the sequential reactions of gap filling, RNA primer removal, and DNA ligation during Okazaki fragment maturation. When the assay was conducted *in vitro*, nuclear extracts from PCNA-K248A–expressing cells showed significant decrease in removing RNA primer flaps and some extent of defect in DNA ligation (Fig. 4E), indicating that the methylation defect of PCNA retarded Okazaki fragment maturation. Defects in the Okazaki fragment maturation process during DNA replication or defects in ligation during DNA repair could lead to accumulation of DNA double-strand breaks (26, 27). To examine the levels of double-strand breaks, 293 cells expressing wild-type and methylation-inactive mutant PCNA were treated with H_2O_2 to determine the survival rate (Supplementary Fig. S11). Consistent with previous data, methylation-inactive mutant PCNA–expressing cells were more sensitive to H_2O_2.

SETD8 and PCNA are coexpressed in lung cancer tissues, and lysine 248 methylation of PCNA promotes the proliferation of cancer cells

We then compared the methylation of endogenous PCNA in normal and cancer cell lines. PCNA was significantly methylated in various types of cancer cell lines, whereas no detectable level of PCNA methylation was found in normal cell lines (Fig. 5A). We subsequently conducted the immunopathologic analysis on clinical lung tissues, analyzing the correlation between SETD8 and PCNA protein expression levels (Fig. 5B). Clinical information and staining patterns of clinical tissues are described in Table 1 and Supplementary Table S6. We found

Table 1. Association between SETD8 and PCNA in lung cancer tissues and patients' characteristics (N = 64)

	Number of cases	SETD8 expression positive	SETD8 expression negative	PCNA expression positive	PCNA expression negative
	n = 64	*n* = 42	*n* = 22	*n* = 48	*n* = 16
Gender	62	40	22	46	16
Male	40	25	15	32	8
Female	22	15	7	14	8
Age, y	62	40	22	46	16
<65	42	28	14	32	10
≥65	20	12	8	14	6
Histologic type	64	42	22	48	16
ADC	14	10	4	10	4
SCC	30	17	13	20	10
Others[a]	20	15	5	18	2
pT factor	63	42	21	48	15
pT0	4	3	1	3	1
pT1	7	7	0	7	0
pT2	41	25	16	29	12
pT3	11	7	4	9	2
pN factor	59	40	19	44	15
N0	48	33	15	34	14
N1	11	7	4	10	1
M factor	61	41	20	46	15
M0	59	40	19	44	15
M1	2	1	1	2	0

Abbreviations: ADC, adenocarcinoma; ASC, adenosquamous-cell carcinoma; LCC, large cell carcinoma; SCC, squamous cell carcinoma.

[a]Others include SCLC, LCC, and ASC.

Published OnlineFirst May 3, 2012; DOI: 10.1158/0008-5472.CAN-11-3701

a correlation factor (ρ) of 0.55378 with P value of 2.068×10^{-6} (by Spearman correlation coefficient) in a cohort of 64 cases (Fig. 5C); lung adenocarcinoma showed a stronger correlation ($\rho = 0.79596$, $P = 3.857 \times 10^{-4}$), supporting our hypothesis that SETD8 overexpression stabilizes and increases the PCNA protein expression in cancer cells. Finally, we examined the effect of PCNA methylation on the growth of cancer cells (Fig. 5D and E). Methylation-inactive–type PCNA–expressing HeLa cells (HeLa-PCNA-K248A) showed a slower growth rate than those with wild-type PCNA–expressing HeLa cells (HeLa-PCNA-WT). Furthermore, to exclude the effect of endogenous PCNA proteins, we first knocked down *PCNA* gene expression, and then, conducted a clonogenecity assay of HeLa cells overexpressing wild-type PCNA and methylation-inactive-type PCNA (Supplementary Fig. S12). Consistent with our previous data, wild-type PCNA showed higher growth promoting effects than methylation-inactive type PCNA. Taken together, these results imply that methylation of PCNA is likely to play a crucial role in the growth promotion of cancer cells.

Discussion

Histone lysine methylation plays a central epigenetic role in the organization of chromatin domains and the regulation of gene expression. We previously reported that the HKMT SMYD3 stimulates cell proliferation through its methyltransferase activity and plays a crucial role in human carcinogenesis (28, 29). Of the various posttranslational protein modifications, the role of protein methylation in signal transduction has not been well characterized. While the carboxyl group and arginine methylation have been implicated in several cellular responses, including receptor signaling, protein transport, and transcription (30), lysine methylation has been considered to be histone specific (31). In the present study, we found that the HKMT SETD8 is overexpressed in various types of cancer and regulates PCNA functions through the methylation of lysine 248. This is a new mechanism revealing the importance of lysine methylation in nonhistone proteins in human cancer.

PCNA was originally reported to be a DNA-sliding clamp for replicative DNA polymerases and is an essential component of the eukaryotic chromosomal DNA replisome (32, 33). It interacts with multiple partners including proteins involved in Okazaki fragment processing, DNA repair, DNA synthesis, DNA methylation, chromatin remodeling, and cell-cycle regulation (34). PCNA has been reported to be modified by ubiquitination, SUMOylation, phosphorylation, and acetylation (9, 11, 12, 35, 36) but its lysine methylation has never been. These kinds of protein modifications are vital for a wide variety of PCNA functions. As reported here, PCNA protein is stably overexpressed in various types of cancer cells, together with SETD8 protein, indicating that SETD8-dependent methylation of PCNA enhances its biologic activity. Knockdown of SETD8 significantly suppressed the growth of cancer cells by diminishing PCNA methylation and reduction of its protein levels. It has been recently reported that knockdown of SETD8 leads to several aberrant phenotypes, including DNA damage, S-phase arrest, and global chromosome condensation (20, 37, 38), consistent with our findings, which suggest that these abnormalities is likely to be caused by dysfunction of the PCNA protein.

PCNA is also considered to be the crucial factor in maintaining the balance between survival and cell death. For instance, PCNA displays an apoptotic activity through interaction with proteins belonging to the Gadd45 family (Gadd45, Myd118, and CR6), which was involved in growth control, apoptosis, and DNA repair (39, 40). Lack of SETD8 induces an increase of the sub-G_1 population of cancer cells (Fig. 1D), so it is possible that apoptosis may be induced by SETD8 depletion through dysfunction of PCNA. Furthermore, we clarified that methylation of PCNA is critical for the interaction with FEN1. It has been reported that FEN1 forms distinct protein complexes for DNA replication and repair. Through its interaction with PCNA, FEN1 is recruited to the replication foci for RNA primer removal and to repair sites for DNA base excision repair (41). Recently, the FEN1–PCNA interaction has been implicated in coordinating the sequential action of polymerase δ (Pol δ), FEN1, and DNA ligase 1 (Lig1) during Okazaki fragment maturation (24). Disruption of PCNA–FEN1 interaction impairs Okazaki fragment ligation (24). We showed that methylation-defective PCNA retards both Okazaki fragment maturation and DNA replication, and induces DNA damages. Cells expressing methylation-inactive mutant PCNA were more sensitive to DNA damage. Because deregulation of FEN1 nuclease has also been reported to be linked to human cancer (42), it is possible that abnormal interactions between FEN1 and PCNA may cause human carcionogenesis. Intriguingly, Guo and colleagues recently showed that methylation of FEN1 suppresses nearby phosphorylation and facilitates PCNA binding (43). Together with our result, this implicates methylation as the crucial player in the interaction between PCNA and FEN1 proteins.

In conclusion, as expression levels of *SETD8* in normal tissues are significantly low (Supplementary Fig. S13), an inhibitor targeting its enzymatic activity might be an effective drug for cancer therapy. Further functional analysis will explore the SETD8-dependent PCNA methylation pathway as a therapeutic target in various types of cancer.

Disclosure of Potential Conflicts of Interest

Y. Yamane, Y. Iwai, and K. Maejima are employed as Researchers in OncoTherapy Science, Inc. R. Hamamoto is a scientific advisor in OncoTherapy Science, Inc. The other authors disclosed no potential conflicts of interest.

Authors' Contributions

Conception and design: M. Takawa, H.-S. Cho, S. Hayami, G. Toyokawa, M. Sugiyama, Y. Nakamura, R. Hamamoto

Development of methodology: M. Takawa, H.-S. Cho, S. Hayami, K. Ueda, N. Dohmae, R. Hamamoto

Acquisition of data (provided animals, acquired and managed patients, provided facilities, etc.): M. Takawa, M. Kogure, K. Ueda, A. Masuda, N. Dohmae, B.A.J. Ponder, R. Hamamoto

Analysis and interpretation of data (e.g., statistical analysis, biostatistics, computational analysis): M. Takawa, H.-S. Cho, M. Kogure, Y. Yamane, Y. Iwai, K. Maejima, K. Ueda, A. Masuda, N. Dohmae, T. Tsunoda, T. Akasu, M. Sugiyama, R. Hamamoto

Writing, review, and/or revision of the manuscript: M. Takawa, H.-S. Cho, K. Ueda, H.I. Field, T. Akasu, S. Ohnuma, Y. Nakamura, R. Hamamoto

Published OnlineFirst May 3, 2012; DOI: 10.1158/0008-5472.CAN-11-3701

Administrative, technical, or material support (i.e., reporting or organizing data, constructing databases): M. Takawa, H.-S. Cho, Y. Yamane, Y. Iwai, K. Maejima, M. Sugiyama, R. Hamamoto
Study supervision: M. Takawa, M. Sugiyama, Y. Atomi, S. Ohnuma, B.A.J. Ponder, R. Hamamoto

Acknowledgments

The authors thank Kazuyuki Hayashi, Noriko Ikawa, and Haruka Sawada for technical assistance.

Grant Support

This work was supported by Grant-in Aid for Young Scientists (A; 22681030) from the Japan Society for the Promotion of Science.

The costs of publication of this article were defrayed in part by the payment of page charges. This article must therefore be hereby marked *advertisement* in accordance with 18 U.S.C. Section 1734 solely to indicate this fact.

Received November 8, 2011; revised April 24, 2012; accepted April 25, 2012; published OnlineFirst May 3, 2012.

References

1. Jenuwein T, Allis CD. Translating the histone code. Science 2001;293:1074–80.
2. Volkel P, Angrand PO. The control of histone lysine methylation in epigenetic regulation. Biochimie 2007;89:1–20.
3. Stoimenov I, Helleday T. PCNA on the crossroad of cancer. Biochem Soc Trans 2009;37:605–13.
4. Miyachi K, Fritzler MJ, Tan EM. Autoantibody to a nuclear antigen in proliferating cells. J Immunol 1978;121:2228–34.
5. Bravo R, Fey SJ, Bellatin J, Larsen PM, Celis JE. Identification of a nuclear polypeptide ("cyclin") whose relative proportion is sensitive to changes in the rate of cell proliferation and to transformation. Prog Clin Biol Res 1982;85:235–48.
6. Celis JE, Bravo R, Larsen PM, Fey SJ. Cyclin: a nuclear protein whose level correlates directly with the proliferative state of normal as well as transformed cells. Leuk Res 1984;8:143–57.
7. Prelich G, Tan CK, Kostura M, Mathews MB, So AG, Downey KM, et al. Functional identity of proliferating cell nuclear antigen and a DNA polymerase-delta auxiliary protein. Nature 1987;326:517–20.
8. Tan CK, Castillo C, So AG, Downey KM. An auxiliary protein for DNA polymerase-delta from fetal calf thymus. J Biol Chem 1986;261: 12310–6.
9. Hoege C, Pfander B, Moldovan GL, Pyrowolakis G, Jentsch S. RAD6-dependent DNA repair is linked to modification of PCNA by ubiquitin and SUMO. Nature 2002;419:135–41.
10. Bailly V, Lauder S, Prakash S, Prakash L. Yeast DNA repair proteins Rad6 and Rad18 form a heterodimer that has ubiquitin conjugating, DNA binding, and ATP hydrolytic activities. J Biol Chem 1997;272: 23360–5.
11. Wang SC, Nakajima Y, Yu YL, Xia W, Chen CT, Yang CC, et al. Tyrosine phosphorylation controls PCNA function through protein stability. Nat Cell Biol 2006;8:1359–68.
12. Naryzhny SN, Lee H. The post-translational modifications of proliferating cell nuclear antigen: acetylation, not phosphorylation, plays an important role in the regulation of its function. J Biol Chem 2004;279:20194–9.
13. Windecker H, Ulrich HD. Architecture and assembly of poly-SUMO chains on PCNA in *Saccharomyces cerevisiae*. J Mol Biol 2008;376: 221–31.
14. Hayami S, Kelly JD, Cho HS, Yoshimatsu M, Unoki M, Tsunoda T, et al. Overexpression of LSD1 contributes to human carcinogenesis through chromatin regulation in various cancers. Int J Cancer 2011;128: 574–86.
15. Hayami S, Yoshimatsu M, Veerakumarasivam A, Unoki M, Iwai Y, Tsunoda T, et al. Overexpression of the JmjC histone demethylase KDM5B in human carcinogenesis: involvement in the proliferation of cancer cells through the E2F/RB pathway. Mol Cancer 2010;9:59.
16. Wallard MJ, Pennington CJ, Veerakumarasivam A, Burtt G, Mills IG, Warren A, et al. Comprehensive profiling and localisation of the matrix metalloproteinases in urothelial carcinoma. Br J Cancer 2006;94: 569–77.
17. Yoshimatsu M, Toyokawa G, Hayami S, Unoki M, Tsunoda T, Field HI, et al. Dysregulation of PRMT1 and PRMT6, type I arginine methyltransferases, is involved in various types of human cancers. Int J Cancer 2011;128:562–73.
18. Olsburgh J, Harnden P, Weeks R, Smith B, Joyce A, Hall G, et al. Uroplakin gene expression in normal human tissues and locally advanced bladder cancer. J Pathol 2003;199:41–9.
19. Huen MS, Sy SM, van Deursen JM, Chen J. Direct interaction between SET8 and proliferating cell nuclear antigen couples H4-K20 methylation with DNA replication. J Biol Chem 2008;283:11073–7.
20. Jorgensen S, Elvers I, Trelle MB, Menzel T, Eskildsen M, Jensen ON, et al. The histone methyltransferase SET8 is required for S-phase progression. J Cell Biol 2007;179:1337–45.
21. Lieber MR. The FEN-1 family of structure-specific nucleases in eukaryotic DNA replication, recombination and repair. Bioessays 1997;19: 233–40.
22. Waga S, Bauer G, Stillman B. Reconstitution of complete SV40 DNA replication with purified replication factors. J Biol Chem 1994;269: 10923–34.
23. Reagan MS, Pittenger C, Siede W, Friedberg EC. Characterization of a mutant strain of *Saccharomyces cerevisiae* with a deletion of the RAD27 gene, a structural homolog of the RAD2 nucleotide excision repair gene. J Bacteriol 1995;177:364–71.
24. Zheng L, Dai H, Qiu J, Huang Q, Shen B. Disruption of the FEN-1/PCNA interaction results in DNA replication defects, pulmonary hypoplasia, pancytopenia, and newborn lethality in mice. Mol Cell Biol 2007;27: 3176–86.
25. Henneke G, Koundrioukoff S, Hubscher U. Phosphorylation of human Fen1 by cyclin-dependent kinase modulates its role in replication fork regulation. Oncogene 2003;22:4301–13.
26. Soza S, Leva V, Vago R, Ferrari G, Mazzini G, Biamonti G, et al. DNA ligase I deficiency leads to replication-dependent DNA damage and impacts cell morphology without blocking cell cycle progression. Mol Cell Biol 2009;29:2032–41.
27. Tishkoff DX, Filosi N, Gaida GM, Kolodner RD. A novel mutation avoidance mechanism dependent on *S. cerevisiae* RAD27 is distinct from DNA mismatch repair. Cell 1997;88:253–63.
28. Hamamoto R, Furukawa Y, Morita M, Iimura Y, Silva FP, Li M, et al. SMYD3 encodes a histone methyltransferase involved in the proliferation of cancer cells. Nat Cell Biol 2004;6:731–40.
29. Hamamoto R, Silva FP, Tsuge M, Nishidate T, Katagiri T, Nakamura Y, et al. Enhanced SMYD3 expression is essential for the growth of breast cancer cells. Cancer Sci 2006;97:113–8.
30. McBride AE, Silver PA. State of the arg: protein methylation at arginine comes of age. Cell 2001;106:5–8.
31. Lachner M, Jenuwein T. The many faces of histone lysine methylation. Curr Opin Cell Biol 2002;14:286–98.
32. Kelman Z, O'Donnell M. Structural and functional similarities of prokaryotic and eukaryotic DNA polymerase sliding clamps. Nucleic Acids Res 1995;23:3613–20.
33. Wyman C, Botchan M. DNA replication. A familiar ring to DNA polymerase processivity. Curr Biol 1995;5:334–7.
34. Moldovan GL, Pfander B, Jentsch S. PCNA, the maestro of the replication fork. Cell 2007;129:665–79.
35. Arakawa H, Moldovan GL, Saribasak H, Saribasak NN, Jentsch S, Buerstedde JM. A role for PCNA ubiquitination in immunoglobulin hypermutation. PLoS Biol 2006;4:e366.
36. Leach CA, Michael WM. Ubiquitin/SUMO modification of PCNA promotes replication fork progression in *Xenopus laevis* egg extracts. J Cell Biol 2005;171:947–54.
37. Houston SI, McManus KJ, Adams MM, Sims JK, Carpenter PB, Hendzel MJ, et al. Catalytic function of the PR-Set7 histone H4 lysine 20 monomethyltransferase is essential for mitotic entry and genomic stability. J Biol Chem 2008;283:19478–88.

Published OnlineFirst May 3, 2012; DOI: 10.1158/0008-5472.CAN-11-3701

38. Tardat M, Murr R, Herceg Z, Sardet C, Julien E. PR-Set7-dependent lysine methylation ensures genome replication and stability through S-phase. J Cell Biol 2007;179:1413–26.
39. Azam N, Vairapandi M, Zhang W, Hoffman B, Liebermann DA. Interaction of CR6 (GADD45gamma) with proliferating cell nuclear antigen impedes negative growth control. J Biol Chem 2001;276:2766–74.
40. Vairapandi M, Balliet AG, Fornace AJ Jr, Hoffman B, Liebermann DA. The differentiation primary response gene MyD118, related to GADD45, encodes for a nuclear protein which interacts with PCNA and p21WAF1/CIP1. Oncogene 1996;12:2579–94.
41. Chen U, Chen S, Saha P, Dutta A. p21Cip1/Waf1 disrupts the recruitment of human Fen1 by proliferating-cell nuclear antigen into the DNA replication complex. Proc Natl Acad Sci U S A 1996;93:11597–602.
42. Zheng L, Jia J, Finger LD, Guo Z, Zer C, Shen B. Functional regulation of FEN1 nuclease and its link to cancer. Nucleic Acids Res 2011;39:781–94.
43. Guo Z, Zheng L, Xu H, Dai H, Zhou M, Pascua MR, et al. Methylation of FEN1 suppresses nearby phosphorylation and facilitates PCNA binding. Nat Chem Biol 2010;6:766–73.

Identification of a novel oncogene, *MMS22L*, involved in lung and esophageal carcinogenesis

MINH-HUE NGUYEN[1], KOJI UEDA[1,4], YUSUKE NAKAMURA[1] and YATARO DAIGO[1-3]

[1]Laboratory of Molecular Medicine, Human Genome Center, Institute of Medical Science, The University of Tokyo, Tokyo; [2]Department of Medical Oncology and [3]Cancer Center, Shiga University of Medical Science, Otsu; [4]Laboratory for Biomarker Development, Center for Genomic Medicine, RIKEN Yokohama Institute, Yokohama, Japan

Received April 27, 2012; Accepted June 12, 2012

DOI: 10.3892/ijo.2012.1589

Abstract. Genome-wide gene expression profile analyses using a cDNA microarray containing 27,648 genes or expressed sequence tags identified *MMS22L* (methyl methanesulfonate-sensitivity protein 22-like) to be overexpressed in the majority of clinical lung and esophageal cancers, but not expressed in normal organs except testis. Transfection of siRNAs against *MMS22L* into cancer cells suppressed its expression and inhibited cell growth, while exogenous expression of MMS22L enhanced the growth of mammalian cells. MMS22L protein was translocated to the nucleus and stabilized by binding to C-terminal portion of NFKBIL2 [nuclear factor of kappa (NFKB) light polypeptide gene enhancer in B-cells inhibitor-like 2]. Expression of a C-terminal portion of NFKBIL2 protein including the MMS22L-interacting site in cancer cells could reduce the levels of MMS22L in nucleus and suppressed cancer cell growth. Interestingly, reduction of MMS22L by siRNAs in cancer cells inhibited the TNF-α-dependent activation of RelA/p65 in the NFKB pathway and expression of its downstream anti-apoptotic molecules such as Bcl-XL and TRAF1. In addition, knockdown of MMS22L expression also enhanced the apoptosis of cancer cells that were exposed to DNA-damaging agents including 5-FU and CDDP. Our data strongly suggest that targeting MMS22L as well as its interaction with NFKBIL2 could be a promising strategy for novel cancer treatments, and also improve the efficacy of DNA damaging anticancer drugs.

Introduction

Lung cancer is the most common cause of cancer-related death, and the worldwide annual death by lung cancer was estimated to be 1.3 million (1). Esophageal squamous cell carcinoma (ESCC) is one of the most common gastrointestinal tract cancers in Asian countries (2). Although a huge body of knowledge about the biology of lung or esophageal carcinogenesis has been accumulated, the development of novel cancer therapeutics remains inefficient to improve patients with these cancers (3). In fact, in spite of development of various molecular targeted therapies, a limited proportion of patients can receive clinical benefit from them (4).

Through genome-wide gene expression analysis of lung and esophageal cancers, we have isolated a number of oncogenes that were involved in the development and/or progression of cancer (5-41). Among the genes upregulated in these cancers, we focused on *MMS22L* (methyl methanesulfonate-sensitivity protein 22-like) which is highly expressed in the majority of clinical lung and esophageal cancers. Our original gene expression profile database also revealed that this gene is highly expressed in clinical cervical cancers, but scarcely expressed in normal tissues except testis, suggesting that *MMS22L* encodes a cancer-testis antigen that can be defined by predominant expression in various types of cancer and undetectable expression in normal tissues except germ cells in testis or ovary (4). Cancer-testis antigens are considered to be good candidate molecular targets for developing new therapeutic strategies for cancers.

Constitutive activation of the NFKB pathway is involved in some forms of cancer such as leukemia, lymphoma, colon cancer and ovarian cancer as well as inflammatory diseases (42-45). The main mechanism of this pathway is reported to be the inactivation of IκB proteins by mutations as well as amplifications and rearrangements of genes encoding the NFKB transcription factor subunits (42-45). However, more commonly it is thought that changes in the upstream pathways that lead to NFKB activation are likely to be aberrantly upregulated in cancer cells (45). Recently some reports suggested that MMS22L-NFKBIL2 interaction could be essential for genomic stability and homologous recombination in immortalized cell lines, suggesting MMS22L to be a new regulator of DNA replication in human cells (46-49). However, no study has indicated critical roles of activation of MMS22L and NFKBIL2 in clinical cancers and investigated their functional importance in carcinogenesis. Here, we report that MMS22L is involved

Correspondence to: Professor Yataro Daigo, Department of Medical Oncology, Shiga University of Medical Science, Seta Tsukinowa-cho, Shiga 520-2192, Otsu, Japan
E-mail: ydaigo@ims.u-tokyo.ac.jp

Key words: MMS22L, oncogenes, therapeutic target, lung cancer, esophageal cancer

in NFKB pathway in cancer cells through its interaction with NFKBIL2 and might be a promising target for development of novel cancer therapy.

Materials and methods

Cell lines and clinical samples. The 12 human lung-cancer cell lines used for in this study included nine NSCLC cell lines (A549, NCI-H1373, LC319, NCI-H1781, PC-14, NCI-H358, NCI-H2170, NCI-H520 and LU61) and three small-cell lung cancer (SCLC) cell lines (SBC-3, SBC-5 and DMS114). The 9 human esophageal carcinoma cell lines used in this study were as follows: eight SCC cell lines (TE1, TE3, TE8, TE9, TE10, TE12, TE13 and TE15) and one adenocarcinoma (ADC) cell line (TE7). A cervical cancer cell line HeLa was also included in the study. All cells were grown in monolayers in appropriate media supplemented with 10% fetal calf serum (FCS) and were maintained at 37˚C in an atmosphere of humidified air with 5% CO_2. Human airway epithelial cells, SAEC (Cambrex Bio Science Inc.), were also included in the panel of the cells used in this study. Primary lung and esophageal cancer samples had been obtained earlier with informed consent (5-10). This study and the use of all clinical materials mentioned were approved by individual institutional ethics committees.

Semiquantitative RT-PCR. We prepared appropriate dilutions of each single-stranded cDNA prepared from mRNAs of clinical lung and esophageal cancer samples, taking the level of β-actin (*ACTB*) expression as a quantitative control. The primer sets for amplification were as follows: *ACTB*-F (5'-GAGGTGATAGCA TTGCTTTCG-3') and *ACTB*-R (5'-CAAGTCAGTGTACAGG TAAGC-3') for *ACTB*, *MMS22L*-F (5'-GTCTCACCTTGGAC AGATGG-3') and *MMS22L*-R (5'-CCAAGGATCCTATTACA CAGTTGC-3') for *MMS22L*. All reactions involved initial denaturation at 95˚C for 5 min followed by 22 (for *ACTB*) or 30 (for *MMS22L*) cycles of 95˚C for 30 sec, 56˚C for 30 sec, and 72˚C for 60 sec on a GeneAmp PCR system 9700 (Applied Biosystems).

Northern blot analysis. Human multiple-tissue northern blots (16 normal tissues including heart, brain, placenta, lung, liver, skeletal muscle, kidney, pancreas, spleen, thymus, prostate, testis, ovary, small intestine, colon, leukocyte; BD Biosciences Clontech) were hybridized with a ^{32}P-labeled PCR product of *MMS22L*. The partial-length cDNA of *MMS22L* was prepared by RT-PCR using primers *MMS22L*-F1 (CTGGAAGAGGCA GTTGAAAA) and *MMS22L*-R1 (ATCGCCCAATATACTG CTCA). Prehybridization, hybridization, and washing were performed according to the supplier's recommendations. The blots were autoradiographed with intensifying screens at -80˚C for 7 days.

Anti-MMS22L antibody. Synthesized peptide with the amino acids sequence of CLGQMGQDEMQRLENDNT [1227-1243] (Cysteine was added to the N-terminal) was inoculated into rabbits; the immune sera were purified on affinity columns according to standard methodology. Affinity-purified anti-MMS22L antibodies were used for western blot as well as immunocytochemical analyses. We confirmed that the antibody was specific to MMS22L on western blots using lysates from cell lines that had been transfected with MMS22L expression vector as well as those from lung and esophageal cancer cell lines that endogenously expressed MMS22L or not.

Western blot analysis. Cells were lysed in lysis buffer; 50 mM Tris-HCl (pH 8.0), 150 mM NaCl, 0.5% NP-40, 0.5% deoxycholate-Na, 0.1% SDS, plus protease inhibitor (Protease Inhibitor Cocktail Set III; Calbiochem). We used ECL western blot analysis system (GE Healthcare Bio-Sciences), as described previously (11).

Immunocytochemical analysis. Cultured cells were washed twice with PBS(-), fixed and rendered permeable in 1:1 acetone: methanol solution for 10 min at -20˚C. Prior to the primary antibody reaction, cells were covered with blocking solution [5% bovine serum albumin in PBS(-)] for 10 min to block non-specific antibody binding. After the cells were incubated with a rabbit polyclonal antibody to human MMS22L (generated to synthesized peptide MMS22L; please see above) or a mouse monoclonal antibody to human NFKBIL2 (Abnova), the Alexa Fluor 488-labelled donkey anti-rabbit secondary antibody (Molecular Probes) or Alexa Fluor 594-labbelled donkey anti-mouse secondary antibody (Molecular Probes) was added to detect endogenous MMS22L or NFKBIL2, individually. Nuclei were stained with 4',6-diamidino-2-phenylindole (DAPI). The antibody-stained cells were viewed with a laser-confocal microscope (TSC SP2 AOBS; Leica Microsystems).

RNA interference assay. Two independent siRNA oligonucleotides against *MMS22L* were designed using the *MMS22L* sequences (GenBank accession no: NM198468). Each siRNA (600 pM) was transfected into two NSCLC cell lines, LC319 and A549 or a cervical cancer cell line HeLa using 30 μl of lipofectamine 2,000 (Invitrogen) following the manufacturer's protocol. The transfected cells were cultured for seven days. Cell numbers and viability were measured by Giemsa staining and 3-(4,5-dimethylthiazol-2-yl)-2,5-diphenyltetrazolium bromide (MTT) assay in triplicate (cell counting kit-8 solution; Dojindo Laboratories). The siRNA sequences used were as follows: control-1 (si-LUC: luciferase gene from *Photinus pyralis*), 5'-CGUACGCGGAAUACUUCGA-3'; control-2 (CNT: On-TARGETplus siControl non-targeting siRNAs of a pool of four oligosnucleotides: 5'-UGGUUUACAUGUCGACUAA-3'; 5'-UGGUUUACAUGUUUUCUGA-3'; 5'-UGGUUUACAUG UUUUCCUA-3'; and 5'-UGGUUUACAUGUUGU GUGA-3'); siRNA-MMS22L-#1 (si-MMS22L-#1: 5'-CCGCCAAUAUCA UCUCUAAUU-3'); siRNA-MMS22L-#2 (si-MMS22L-#2: 5'-GAA CCUGCAAUACAUGGUAUU-3'). Downregulation of endogenous MMS22L expression in the cell lines by siRNAs for *MMS22L*, but not by controls, was confirmed by semiquantitative RT-PCR and western blot analyses.

Cell growth assay. COS-7 or HEK293 cells that express endogenous *MMS22L* at a very low level were transfected with mock or MMS22L-expressing vectors (pCAGGSn-3xFlag-MMS22L) using lipofectamine 2,000 transfection reagent (Roche). Transfected cells were incubated in the culture medium containing 0.8 mg/ml neomycin (Geneticin, Invitrogen) for 7 days. Expression of MMS22L as well as viability and colony numbers of cells were evaluated by western blot analysis, and MTT and colony-formation assays at day 7.